

Review

The Application of Metal–Organic Frameworks in Water Treatment and Their Large-Scale Preparation: A Review

Yuhang Xie ^{1,2}, Teng Zhang ^{1,2,3,*}, Bo Wang ^{1,2} and Wenju Wang ^{4,*}

- ¹ Frontiers Science Center for High Energy Material, Beijing Key Laboratory of Photoelectronic Ministry of Education, Advanced Research Institute of Multidisciplinary Science, School of Chemistry and Chemical Engineering, Beijing Institute of Technology, Beijing 100081, China; xyh1654228985@163.com (Y.X.); bowang@bit.edu.cn (B.W.)
- ² Conversion Materials, Key Laboratory of Cluster Science, Ministry of Education, Advanced Research Institute of Multidisciplinary Science, School of Chemistry and Chemical Engineering, Beijing Institute of Technology, Beijing 100081, China
- ³ Advanced Technology Research Institute (Jinan), Beijing Institute of Technology, Jinan 250300, China
- ⁴ School of Energy and Power Engineering, Nanjing University of Science and Technology, Nanjing 210094, China
- * Correspondence: zhanghaiteng11@163.com (T.Z.); wangwenju@njust.edu.cn (W.W.)

Abstract: Over the last few decades, there has been a growing discourse surrounding environmental and health issues stemming from drinking water and the discharge of effluents into the environment. The rapid advancement of various sewage treatment methodologies has prompted a thorough exploration of promising materials to capitalize on their benefits. Metal–organic frameworks (MOFs), as porous materials, have garnered considerable attention from researchers in recent years. These materials boast exceptional properties: unparalleled porosity, expansive specific surface areas, unique electronic characteristics including semi-conductivity, and a versatile affinity for organic molecules. These attributes have fueled a spike in research activity. This paper reviews the current MOF-based wastewater removal technologies, including separation, catalysis, and related pollutant monitoring methods, and briefly introduces the basic mechanism of some methods. The scale production problems faced by MOF in water treatment applications are evaluated, and two pioneering methods for MOF mass production are highlighted. In closing, we propose targeted recommendations and future perspectives to navigate the challenges of MOF implementation in water purification, enhancing the efficiency of material synthesis for environmental stewardship.



Citation: Xie, Y.; Zhang, T.; Wang, B.; Wang, W. The Application of Metal–Organic Frameworks in Water Treatment and Their Large-Scale Preparation: A Review. *Materials* **2024**, *17*, 1972. <https://doi.org/10.3390/ma17091972>

Academic Editor: Valentina Gargiulo

Received: 10 March 2024

Revised: 5 April 2024

Accepted: 11 April 2024

Published: 24 April 2024



Copyright: © 2024 by the authors. Licensee MDPI, Basel, Switzerland. This article is an open access article distributed under the terms and conditions of the Creative Commons Attribution (CC BY) license (<https://creativecommons.org/licenses/by/4.0/>).

1. Introduction

In recent years, pollution has surged, becoming a formidable adversary to freshwater ecosystems, the atmosphere, and human well-being [1–3]. The infiltration of heavy metals such as arsenic (III), lead (II), and mercury (II), alongside a variety of organic pollutants ranging from dyes and pesticides to endocrine disruptors and pharmaceuticals, has raised global alarms [4–7]. It has been demonstrated that that traditional wastewater treatment has many shortcomings. For example, the removal capacity of high-concentration organic pollutants, micro-pollutants, high-salt wastewater and nitrogen and phosphorus is limited, and the resource utilization capacity is weak. Even trace levels of these contaminants remaining in water can cause adverse health effects, including skin damage, infectious diseases, acute or chronic poisoning, and so on [8]. The advent of metal–organic frameworks (MOFs) has opened new horizons in combating these pollutants [9–11]. These structures, with their metal nodes interconnected by organic ligands, create a range of porous geometries from one to three dimensions [12–14]. Their robust crystalline frameworks offer

unmatched porosity and vast surface areas, which have ushered them into a plethora of applications such as gas storage, chemical catalysis, and environmental clean-up, to name a few. The ultrahigh porosity and larger specific surface area of MOFs have significantly contributed to their wide applications in luminescence, gas storage, chemical catalysis, gas adsorption, biomedical imaging, catalytic degradation, energy generation, and environmental remediation [9,14–16]. Regarding pollutant removal, recent review papers have detailed the environmental applications of MOFs, primarily focusing on the adsorption of diverse contaminants (e.g., organics, heavy metals, and toxic gases) and catalytic eliminations of various water pollutants through methods such as Fenton-like oxidation [17], photocatalysis [18], electrocatalysis [19], and sulfate radicals-based reactions [20]. These studies consistently propose that MOFs can serve as effective and re-cyclable materials for pollution remediation.

While metal–organic frameworks (MOFs) offer significant benefits, their application in environmental management is not without challenges [21–23]. Firstly, the water stability and biocompatibility of MOFs themselves hinder the use of some MOFs on an industrial scale. Secondly, MOFs in powdered form are susceptible to quick depletion when used practically, leading to reduced longevity and higher operational costs. Thirdly creating multifunctional MOFs with precise control over their size, shape, and selectivity is a complex process. Achieving cost-effective, large-scale production for industrial use remains a demanding task requiring further innovation. To leverage the full potential of MOFs and overcome these practical hurdles, innovative large-scale production methods have been introduced. These include electrochemical [24], microwave [25], and mechanochemical [26] techniques, along with newer methods such as spray drying [27], flow chemistry [28], and high-pressure homogenization [29]. These advancements hold promise for refining MOF production and making their exceptional properties more accessible for widespread industrial application. However, currently, the materials suitable for achieving large-scale preparation are still limited, and in the actual application process, the integrity of the large-scale MOF preparation process needs improvement.

Based on this, this review tries to integrate all current MOF-related water treatment methods so that readers can have a comprehensive understanding of this (Figure 1). It is worth mentioning that this also includes the detection technology of MOF-related pollutants, and gives practical recommendations from the raw material production side. In this way, the comprehensive application of MOF in the field of water treatment from production to water quality testing to sewage treatment is promoted.

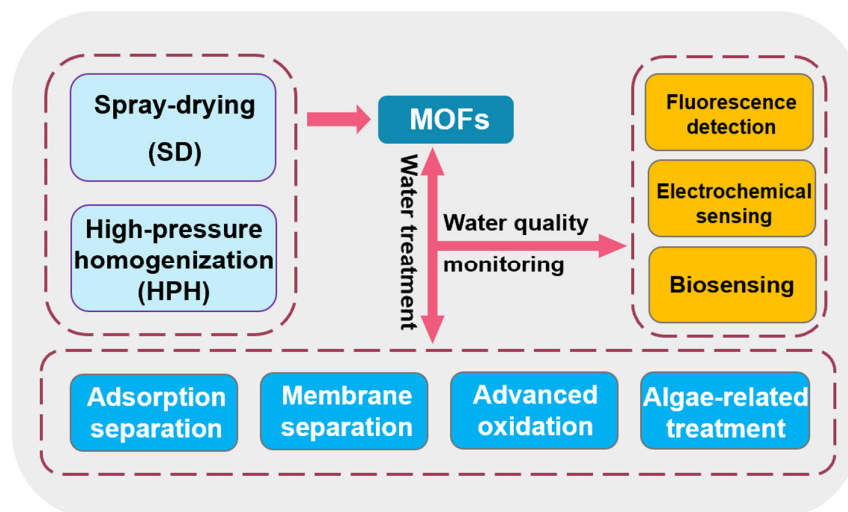


Figure 1. Summary content structure diagram.

2. MOF-Based Water Treatment Strategy

2.1. Separation Method for the Treatment of Pollutants in Water

2.1.1. Adsorption Separation

Adsorption emerges as a leading technique in water pollution control due to its simplicity, cost-effectiveness, and high efficiency [30–32]. Nevertheless, traditional adsorbents for inorganic contaminants (IOCs) often suffer from inherent limitations such as inadequate adsorption capacity, non-selective adsorption, and subpar recyclability [33]. To overcome these barriers, innovative adsorbents are being actively pursued. MOFs, with their impressive capabilities, are at the forefront of this research. Four common MOF adsorptive modes for IOCs include van der Waals force, electrostatic interaction, ion exchange, and coordination binding (Figure 2). A notable study by Lv et al. [34] highlighted a hydrothermally synthesized Ni-MOF with a high affinity for arsenic (V), where adsorption capacity was optimally enhanced at 454.94 mg/g by balancing van der Waals forces with the density of oxygen-containing functional groups after pyrolysis at 400 °C. Similarly, the removal of emerging organic contaminants by MOFs involves diverse interactions such as electrostatic, hydrophobic, acid-base, p-p interactions, hydrogen bonding, and coordination binding [35–40]. In a remarkable study, Seo et al. [41] utilized the p-p and electrostatic interactions within UiO-66 to capture methylchlorophenoxy propionic acid from water, boasting an adsorption efficiency nearly 30 times greater than that of activated carbon.

And to sum up the latest research, UiO series and MIL series are still the most commonly used MOF systems for adsorption and removal of water pollutants. For example, experimental data in the recent work of D et al. [42] show that the metal–organic skeleton of UiO-66-NH₂ can effectively remove fluoride ions present in industrial wastewater (using 100 mg of MOF in 50 mL industrial wastewater to remove 70–80% of fluoride in 60 min). The MIL series has also been recently summarized in the related literature [43]. It is important to acknowledge that the widespread adoption of these MOFs in water purification is largely due to their superior water stability. Generally, MOFs exhibit robust water stability under conditions such as the presence of metal ions with large atomic radii and low ionization potentials, or ligands with fewer six-membered rings and additional cyclic bivalent nodes. Furthermore, the advent of machine learning in research offers a new avenue for predicting the water stability of MOFs with greater ease [44].

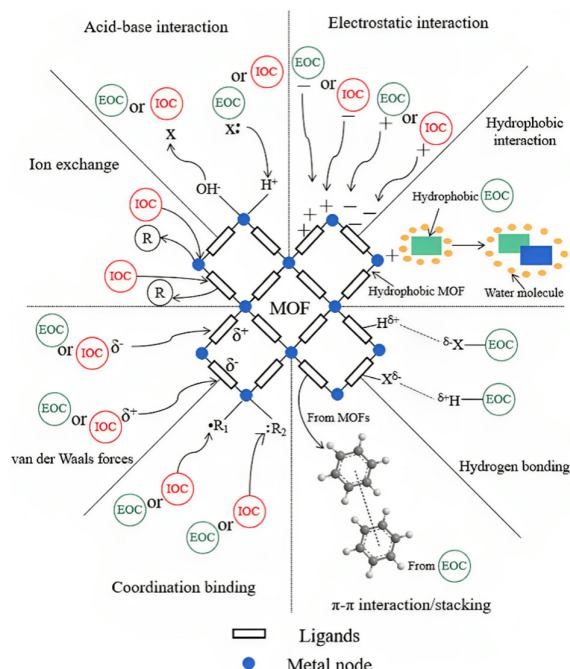


Figure 2. Schematic diagram of possible mechanisms for adsorptive removal of contaminants over MOFs [45].

While MOFs hold promise as superior adsorbents, their transition from laboratory to market is impeded by economic constraints. The raw materials for MOFs are relatively inexpensive, yet commercial procurement costs far exceed those of conventional adsorbents such as activated carbon and zeolite [46–50]. This discrepancy stems from the predominant synthesis technique for MOFs—solvothermal methods—which are notably laborious, reliant on organic solvents, and necessitate intricate purification processes. These factors cumulatively inflate production costs, rendering MOFs less commercially viable. Furthermore, balancing the adsorption efficacy against the manufacturing expense poses an ongoing challenge. Notwithstanding these production hurdles, the sorbent market is witnessing robust growth, as underscored by the “Global Economy of Sorbents 2024” report. This report documents a market expansion from USD 4.67 billion in 2023 to an estimated USD 5 billion in 2024, reflecting a healthy compound annual growth rate of 7.0%. Such growth indicates vigorous efforts to innovate and expand the portfolio of available adsorbents, hinting at the potential for MOFs to capture a share of this expanding market once economical production barriers are surmounted.

2.1.2. Membrane Separation

In addition to adsorption separation, membrane technology, leveraging the principles of size exclusion and adsorption, has emerged as a highly effective and convenient approach for the one-step removal of aquatic contaminants [51]. The integration of MOFs into composite membranes capitalizes on their distinct characteristics—such as tunable modularity, functionality, vast surface area, and porous structure [23]. Various strategies for preparing nanoMOF-based composite membranes are summarized in Table 1. For instance, biocompatible and renewable cellulose is an excellent substrate/matrix for compositing MOFs. Abdelhameed et al. [52] demonstrated this by coating Cu-BTC (1,3,5-Benzenetricarboxylic acid) onto cotton fabrics and applied it for organophosphate insecticide pollution remediation. The Cu-BTC@cotton composite showed a maximum ethion adsorption capacity of 182.0 mg g^{-1} and followed the Langmuir model. In a similar vein, Schelling et al.’s functionalization of cotton fabrics with UiO-66 showcased its efficacy in herbicide adsorption [53]. Table 2 presents a curated selection of 15 research studies from the last one to two years on MOF composite membranes used in water treatment, chosen for their distinctive surface properties. These are intended to provide readers with fresh perspectives and spark innovative developments in the field.

Moreover, most dyes are eliminated onto membranes containing MOFs through electrostatic interactions [54–56]. In addition to the advantages of using MOF-containing membranes to eliminate dyes, practical applications still pose a huge challenge due to their stability in wastewater and lack of robustness in complex pollutants present in water environments. In addition, research on the effects of coexisting ions and operating modes on the elimination of dyes in wastewater is very limited. Therefore, in-depth research on the factors and reaction mechanisms that affect dye removal is crucial for enhancing the sustained application of MOF-containing membranes in dye decontamination. Similarly, in terms of removing heavy metal pollutants, membranes containing MOFs have the characteristics of fast equilibrium time, strong removal ability, and high selectivity towards target heavy metal ions, and can maintain excellent performance even under extreme environmental conditions [57–60]. To our knowledge, the reaction mechanism is mainly attributed to electrostatic interactions and pore-filling effects. However, most current research has focused on selectively eliminating a target ion, and the actual water environment is complex and variable. Therefore, further research on the simultaneous treatment of multiple pollutants by MOF-containing membranes is of great significance for actual wastewater purification.

Table 1. Various strategies for the preparation of nanoMOF-based composite membranes.

Membrane Type	Strategy	Unique Characteristics	References
TFN	Integrating MOF nanoparticles within the polyamide (PA) layer is deftly achieved using the interfacial polymerization (IP) process	PA layer can be tailored, affecting factors such as the degree of cross-linking and the layer's thickness. These modifications have the potential to enhance the layer's permeability to water and, in certain instances, can also improve its selectivity in terms of solute rejection.	[61]
	Applying a layer of nanoMOFs onto the PA layer	Modifying a membrane's surface can alter its hydrophilicity and charge, which can introduce or enhance antifouling and antibacterial properties. Such enhancements are integral to developing durable membranes that maintain high separation efficiency over extended periods.	[62]
MMM	Embedding MOF nanoparticles into the matrix of a substrate or a single-layer membrane	Adjusting the fabrication parameters of a membrane offers the potential to enhance its porosity and reduce both its thickness and the complexity of its internal pathway, known as tortuosity. These modifications could lead to a reduced structural parameter (S-value) and an increased water flux, thereby optimizing the membrane's filtration performance.	[63]
Others	Incorporating water unstable MOF nanoparticles as pore formers in the fabrication of membranes can create a network of pores	By calibrating the size of the nanoparticles used in membrane construction, it is feasible to enhance membrane porosity and precisely control the mean pore size. This approach can be undertaken without altering the inherent chemical properties of the membrane, such as hydrophilicity and surface charge, maintaining its functional integrity while optimizing its physical structure for improved performance.	[64]
	Creating a selective layer of nanoMOFs on a substrate	Advancements in membrane technology offer the potential to augment the mechanical durability of membranes, precisely tailor surface physicochemical characteristics—including hydrophilicity, electrical charge, and surface roughness—and amplify selectivity, particularly in nanofiltration (NF) and membrane distillation (MD) processes. These enhancements can lead to more resilient and efficient filtration systems.	[65]

Table 2. Summary of the latest research results of water treatment MOF composite membranes.

Membrane Components		Craft	Target Contaminants	References
1	D ₆ /TiO ₂ /MoS ₂ /NiCo-NC/PVDF	Negative pressure assisted method	Pesticides, pharmaceuticals, Personal physical items	[66]
2	MIL-101(Fe)/Cu-POM/IPN	In-situ deposition, pouring	Dye, Drugs	[67]
3	MOF-5/coal-based fiber	Electrospinning	Dye	[68]
4	FS-50/COF(MATPA)-MOFs(Zr)/PDA@PVDF	High pressure induction	Microplastics, dye, pesticides	[69]
5	CoFe-MOF/TiO ₂ /PVDF	Non-solvent-induced phase separation	Antibiotic	[70]
6	PAN/Co-MOFs	In-situ growth, electrospinning	Dye	[71]
7	MOF/GO	Vacuum filtration	Dye	[72]
8	MOF/PCL	Solvent/non-solvent methods	Dye	[73]
9	PVA/GO/MOF	Chemical crosslinking and suction filtration	Greasy dirt	[74]
10	Co-CAT-1/PEI/GO	Coating process	Greasy dirt	[75]
11	Bio-MOF-2Me/MMM	Pouring	Cationic dyes	[76]
12	CF/PDA/UiO-66-NH ₂	Grown in situ	Rhodamine B and Pb(II) metalions	[77]
13	Ag(I)-CP/PES	Scraper casting	Dye	[78]
14	MOF/PAN-MIM	In-situ deposition	Bisphenol A	[79]
15	MOF-1a/PVDF	Drip casting method	TNP	[80]

PVDF = Polyvinylidene fluoride; IPN = polymer network; PAN = electrospun polyacrylonitrile; GO = graphene oxide; PCL = porous polycaprolactone; PVA = polyvinyl alcohol; PEI = polyethylenimine; PDA = polydopamine; CF = cotton fabric; PES = sensitive polyether sulfone; TNP = harmful nitro explosive.

2.2. Advanced Oxidation

Advanced oxidation processes (AOPs) have emerged as highly effective strategies for contaminant removal, owing to the radicals they generate in situ, such as hydroxyl ($\cdot\text{OH}$), superoxide ($\cdot\text{O}_2^-$), and sulfate ($\cdot\text{SO}_4^{2-}$) radicals. The simplicity of AOP operation, coupled with mild reaction conditions and high efficiency, has garnered significant interest in recent years [81,82]. The potent oxidizing nature of these radicals not only breaks down organic pollutants but also mitigates their toxicity and, in some instances, mineralizes them into CO₂ [83,84]. Photocatalysis, Fenton and Fenton-like reactions, electrocatalysis, and ozonation, along with various hybrid techniques, are among the AOPs that have seen

considerable development for water treatment applications [85–88]. In the past decade, the application of iron containing MOFs in heterogeneous Fenton reactions has significantly increased due to their high efficiency. Fe MOFs exhibit a higher tendency for electron hole pair recombination, resulting in lower photocatalytic activity. Nowadays, the use of Fe MOFs and semiconductors to prepare composite materials has been designed as a successful strategy to improve charge transfer efficiency. The metal organic framework group of MIL (Lavoisier Materials Research Institute) is one of the most explored categories of MOFs in the field of environmental remediation [89]. Table 3 summarizes some representative studies of MOF (Fe)-based catalysts.

In addition, the latest results show that MOF-derived carbon nanomaterials can avoid the inherent shortcomings of MOF precursors while giving full play to their advantages, and their outstanding performance in the field of AOP water treatment is the focus of research by scientists. For example, C et al. [90] used polydopamine-modified MOF-5-derived carbon as a persulfate activator for aniline air flotation (AFF) degradation, achieving effective oxidation of AAF within 30 min. Wu et al. [91] obtained more active sites by pyrolysis of MOF composites (ZIF-67/NG), which effectively activated peroxyomonosulfate tetracycline. Liu et al. [92] using Fe-MOF-derived carbon compounds as catalysts for persulfate oxidative degradation of trichloroethylene, achieved a highest trichloroethylene removal rate of 85.8%. Again, the mechanism involved is the strong oxidation of free radicals, as we have described above, which enables the efficient decomposition of organic pollutants.

Table 3. Selective oxidation of MOF-based catalysts.

Catalyst	Organic Pollutant/Removal Efficiency (%)	Co-Existing Substance/Removal Efficiency (%)	Oxidant/Irrigation	Dominant Mechanism	References
FeCo MOF	CR/95%, RhB/99%, MO/95%, BPA/100%	3-NP/40%, p-BA/50%	PMS	O_2	[93]
Fe-MOF membrane	BPS/75.7%	BA/-	H_2O_2	Size exclusion	[94]
MIL-53(Fe)@anionicresin	MB/84%	SRB/11%	visible light	Electrostatic interaction	[95]
MIL-53(Fe)@anionicresin	SRB/73%	MB/59%	visible light	Electrostatic interaction	[95]
Fe-BTC@resin	MB/71%	SRB/12%	visible light	Electrostatic interaction	[96]
Fe-MOF@MIP	SMX/97%	BA/-	PS	MIT	[97]
Fe-MOF-74@MIP	DMP/95%	DEP/80%, DBP/70%, DEHP/70%	PS	MIT	[98]
Fe-MOF-74@SiO ₂ @MIP	DMP/93%	DEP/68%, OG/18%, SMX/23%	PS	MIT	[99]
Zn ₄ Co ₁ -C yolk-shell Co/C	Phenol/100% BPA/100%	BA/1% BA/-	PMS PMS	O_2 Size exclusion	[100] [101]
Cu/RGO	2,4-DCP/95.8%	BA/0%, CBZ/10%, IBU/30%	PDS	Cu(III)	[102]
Fe/Fe ₃ O ₄ @rGO	BPA/90%, BPF/60%, MeP/12%, p-BA/13%, 2,4-DCP/100%, CP/30%, BPS/12%, phenol/12%	-	PDS	Hydrophobicity	[103]

Note: BTC = 1,3,5-tricarboxylic acid; MIT = molecularly imprinted technology; RhB = rhodamine B; BPA = bisphenol A; BPS = bisphenol S; MB =methylene blue; SMX = sulfamethoxazole; DMP = dimethyl phthalate; 2,4-DCP = 2,4-dichlorophenol; BPF = bisphenol F; p-BA = 4-hydroxybenzaldehyde; CP = 4-chlorophenol; 3-NP = 3-nitrophenol; BA = benzoic acid; IBU = ibuprofen.

2.3. Other MOF-Based Water Treatment Strategies

2.3.1. Acts as a Flocculant to Remove Harmful Algae

In the quest for advanced water treatment solutions, the MIL series of metal–organic frameworks (MOFs) has emerged as particularly promising. Notably, MIL-101 distinguishes itself through its exceptional chemical robustness in various solvents, ease of production, biological compatibility, extensive surface area, and cost-effectiveness [104–106]. For instance, a groundbreaking application proposed by Li et al. [107] leverages MOFs, specifically NH₂-

MIL-101(Cr), as flocculants to address the pervasive issue of harmful algal blooms. Their research revealed that this nanoscale, amine-functionalized chromium-based MOF is particularly effective against *Microcystis aeruginosa*—a dominant and ecologically damaging algae species. This MOF exhibits superior algal removal capabilities, surpassing those of traditional flocculants across a spectrum of environmental conditions, demonstrating a powerful potential for water purification processes. The mechanism behind NH₂-MIL-101(Cr)'s effectiveness is believed to be twofold: firstly, the MOF particles aggregate and attach to the algae cells; subsequently, they co-precipitate, removing the algae from the water. This not only clears the immediate contamination but also helps restore water quality and maintain ecological balance. Despite these advantages, it is imperative to consider the broader implications of introducing such materials into the environment. Potential impacts on water quality, the ecosystem, and public health need thorough assessment to mitigate any risks associated with their use. Responsible application of MOFs, with careful monitoring and adherence to safety guidelines, is essential to harness their benefits without compromising environmental integrity and human well-being.

2.3.2. Inhibit the Growth of Algae

Exploiting the multifaceted advantages of MOFs, various studies have probed their potential in controlling algal proliferation [108–110]. For example, Fan et al. [111] showcased the remarkable algae-inhibiting capabilities of Cu-MOF-74, recording a 75.5% removal rate of algae within 120 h. This significant reduction is partially attributed to a 56% decrease in chlorophyll a content, indicating impairment of the photosystem due to diminished chlorophyll a and phycobiliprotein levels. This damage stems from the sustained release of copper ions (Cu²⁺) from Cu-MOF-74, which serve as a metal ion reservoir, inducing reactive oxygen species (ROS) accumulation within the algal cells. This oxidative stress leads to lipid peroxidation, evidenced by the loss of oxidation balance, decreased superoxide dismutase (SOD) activity, and increased catalase (CAT) activity in the algal cells (Figure 3). In addition, the generation of hydroxyl radicals by Cu-MOF-74 further exacerbates cellular damage, culminating in the death of *Microcystis aeruginosa*. Consequently, the concentration of extracellular organic matter in the water is observed to rise. These findings illuminate the efficacy of copper-based MOFs, not just as inhibitors but also as agents of removal for harmful algal species.

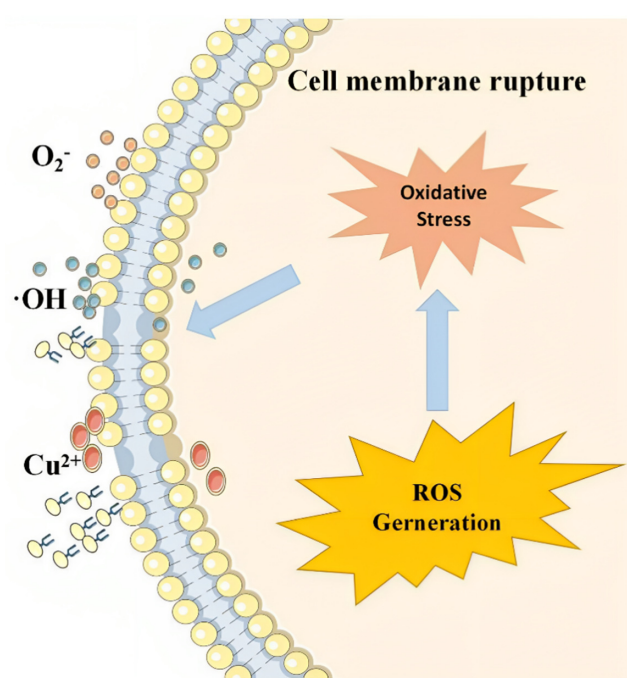


Figure 3. The principle of inhibiting the growth of *M. aeruginosa* by Fe₃–O₄BC@Cu-MOF-74 [89].

2.4. Sensing Monitoring and Detection

The myriad water treatment methodologies utilizing MOFs, as outlined above, highlight the versatility of these materials. Concurrently, the evolution of sensing technologies has paved the way for the use of MOFs in the detection of water quality, adding an additional layer of utility to their application in water management.

Despite the promising nature of these cutting-edge MOF-based technologies, it is important to note that their implementation, whether standalone or in synergy with established methods, is still undergoing preliminary assessment. Nevertheless, available research data suggest that these novel approaches—whether applied individually or in tandem—have already demonstrated effective pollutant mitigation capabilities [112]. In the following sections, we will delve into three pivotal studies that underscore the use of MOFs in both the remediation and monitoring aspects of water treatment, thereby painting a comprehensive picture of their role in ensuring water safety and purity.

2.4.1. Fluorescence Detection

A significant body of early research on MOF-based fluorescence sensors has focused on detecting key pollutants known for their adverse impact on water quality, such as metal ions, anions, and nitroaromatic compounds. These compounds are adept at quenching fluorescence through processes like internal filtering effects (IFE) and photoinduced electron transfer (PET) [113,114]. MOF-based sensors distinguish themselves from other fluorescence sensors crafted from small molecules or conjugated polymers by offering superior chemical tunability, which facilitates precise and efficient host–guest recognition [115–123]. Moreover, the inherent structure of MOFs, laden with numerous π and n electrons, is conducive to producing robust and diverse fluorescence signals [124–126]. This, combined with their capacity to be easily modified and decorated onto various substrates, positions MOFs as particularly promising candidates for fluorescence-based sensing applications [127–131]. Illustrating their potential, Huang et al. [132] reported on the solvothermal synthesis of an Al^{3+} MOF, denoted as CAU-1-(OH)₂, featuring ligands that strongly coordinate with Bi^{3+} due to the hydroxyl and carboxyl groups. This affinity of bismuth for oxygen, which is greater than that of the MOF's metal center, leads to the replacement of Al with Bi, resulting in fluorescence quenching. CAU-1-(OH)₂ showcases the ability to detect Bi^{3+} in water with a remarkably fast response time of 24 s and a detection limit of 2.16 μM . Although its sensitivity to pH may influence detection, this sensor serves as a valuable prototype for future sensor development aimed at Bi^{3+} and possibly other metal ions [133]. Figure 4 shows the different fluorescence signal sources in MOF-based fluorescence sensors.

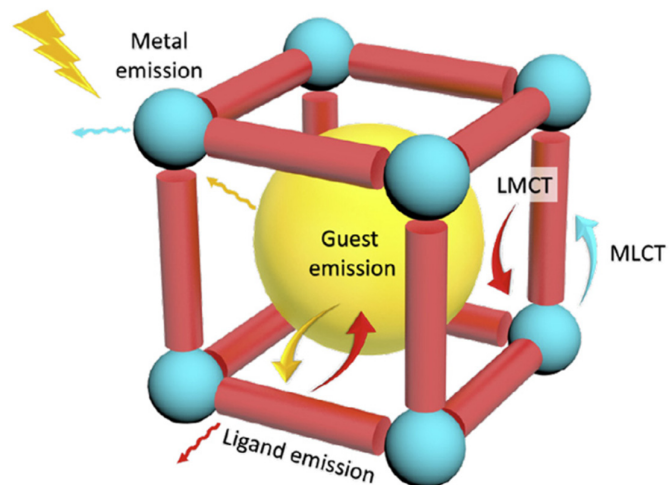


Figure 4. Schematic diagram showing the different sources of fluorescence signals in MOF-based fluorescence sensors [133].

2.4.2. Electrochemical Sensing

In addition to the aforementioned fluorescence detection, the advancements in nanotechnology and functional materials have catalyzed the evolution of electrochemical detection techniques [134,135]. Leveraging their unique structures and properties, these materials provide a solid framework for developing sophisticated electrochemical sensors, particularly for the surveillance of heavy metal ions in various environments [136–139]. Table 4 offers a comprehensive overview of MOF-based electrochemical sensors designed for the detection of transition metal ions. It reveals that the predominant sensing mechanism in these applications is the cation exchange between the metal ions and the MOFs. This exchange mechanism plays a crucial role in the sensor's ability to identify and quantify specific metal ions, underscoring the versatility and effectiveness of MOFs as a key component in environmental monitoring strategies.

Table 4. Recent overview of MOF-based sensors for transition metal ions and their mechanism of sensing.

Transition Metal Ion	MOF-Based Sensor	Detection Mechanism	References
Cr ⁺³	3D Ca-MOF	Competitive absorption mechanism	[140]
Cr ⁺³	Eu-MOF	Cation exchange quenching mechanism	[141]
Cr ⁺³	Eu-MOF	Cation exchange quenching mechanism	[142]
Cr ⁺³	Tb-MOF	Cation exchange quenching mechanism	[142]
Cr ⁺⁶	MOF-199	Oxidoreductase	[143]
Cr ⁺³	MIL53-L	LLCT mechanism	[144]
Cr ⁺³	BPEI-CQDs/ZIF-8-MOFs	Cation exchange quenching effect	[145]
Cr ⁺³	[NH ₄] ₂ [ZnL]-6H ₂ O (Lin et al.) ⁿ	Host-guest Interaction	[146]
Cr ⁺³	Cd-MOF-74	Cation exchange quenching mechanism	[147]
Cr ⁺³	Zn-based HPU-1	PET/FRE mechanism	[148]
Cr ⁺³	2D[Zn ₂ (TPC ₄ A)(DMF)(H ₂ O ₄)] ₃ H ₂ O	Zn-based HPU-1	[149]
Mn ⁺²	MOFs [Zn (dbp)] ⁿ	Cation exchange quenching mechanism	[150]
Mn ⁺²	[Cd (dbp) (H ₂ O)]2H ₂ O·CH ₃ CN) ⁿ	Competitive absorption	[151]
Mn ⁺²	[NH ₄] ₂ [ZnL]-6H ₂ O	Competitive absorption	[152]
Mn ⁺²	MOF-525	Host-guest Interaction	[146]
Mn ⁺²	PCN-222-Pd	Cation exchange quenching mechanism	[153]
Mn ⁺²	3D [[(CH ₃) ₂ NH ₂] ₂ [Zn-(TNC ₄ A)][[(CH ₃) ₂ NH ₂] ₂ [Zn-(TNC ₄ A)]][[(CH ₃) ₂ NH ₂] ₂ [Zn-(TNC ₄ A)]].4H ₂ O	Cation exchange quenching effect	[144]
Fe ⁺³	NNU-1	Cation exchange quenching mechanism	[150]
Fe ⁺³	[Zn ₂ (OBA) ₂ (BPTP)]	Cation exchange quenching effect	[154]
Fe ⁺³	[Ni(OBA) ₂ (BPTP) ₂ (H ₂ O) ₂]	Competitive absorption quenching effect	[155]
Fe ⁺³	[Cd ₂ (OBA) ₂ (BPTP) (H ₂ O) ₂]	Competitive absorption quenching effect	[155]
Fe ⁺³	[Cd(L)(BPDC)](H ₂ O) ₂	Competitive absorption quenching effect	[155]
Fe ⁺³	[Cd(L)(SDBA)(H ₂ O)](H ₂ O) _{0.5}	Competitive absorption quenching effect	[155]
Fe ⁺³	Cd-MOF	FRET/PET mechanism	[156]
Fe ⁺³	BUT-14	RET/FRET mechanism	[156]
Fe ⁺³	BUT-15	RET/FRET mechanism	[156]
Fe ⁺³	UMCM-1-NH ₂	Fluorescence quenching mechanism	[156]
Fe ⁺³	[Cd (5-asbaz (bimb))] ⁿ	FRET/PET mechanism	[156]
Fe ⁺³	3D Tb-MOF	FRET/PET mechanism	[157]
Fe ⁺³	Zirconium MOF	FRET/PET mechanism	[158]
Fe ⁺³	Zn-MOF	LLCT mechanism	[159]
Zn ⁺²	([Ln (PDA) ₃ Mn _{1.5} (H ₂ O) ₃]·3.25H ₂ O	PET/FRET mechanism	[160]
Pd ⁺²	NH ₂ -MIL-53(Cr)	PET/FRET mechanism	[160]
Cd ⁺²	Zn-MOF	LMCT mechanism	[161]
Hg ⁺²	ZnMOF	Cation exchange quenching effect	[162]
Hg ⁺²	EuMOF	PET/FRET mechanism	[163]
Hg ⁺²	RuMOF	PET/FRET mechanism	[164]
Hg ⁺²	Eu/IPA CPNPs	PET/FRET mechanism	[162]
Lanthanides	{[GdIII ₂ L ₆₄)Mn(H ₂ O) ₆]·XH ₂ O} _n	Cation exchange quenching effect	[165]
Lanthanides	CdMOFs	PET/FRET mechanism	[165]
Lanthanides	MgMOF	PET/FRET mechanism	[165]
Miscellaneous Transition Metal Ions	Eu ³⁺ @MIL-121	PET/FRET mechanism	[166]

Table 4. Cont.

Transition Metal Ion	MOF-Based Sensor	Detection Mechanism	References
Miscellaneous Transition Metal Ions	UiO-bpydc	PET/FRET mechanism	[166]
Miscellaneous Transition Metal Ions	Eu-bpydc	PET/FRET mechanism	[166]

Note: H₂dbp = 4'-(4-(3,5-dicarboxyphenoxy)phenyl)-4,2':6',4''-terpyridine; BPEI-CQD = poly-(ethylenimine)-capped carbon; DMF = Dimethyl formamide; TPC = terephthalyl chloride; dbp = dibutyl phthalate; bimb = 4,4' -Bis(1-imidazolyl)biphenyl; BPTP = 3,5-bis(5-(pyridin-4-yl)thiophen-2-yl)pyridine)[Ni(OBA)₂(BPTP)₂(H₂O)₂] and [Cd₂(OBA)₂(BPTP)(H₂O); PDA = p-Phenylenediamine; BPDC = 4,4'-biphenyldicarboxylic acid; SDBA = 4,4'-sulfonyldibenzoic acid; bpydc = 2,2'-bipyridine 5,5'-dicarboxylic acid.

The efficacy of sensors is closely tied to their sensitivity toward the targeted analyte, which in turn is intricately linked to the electrochemical kinetics within the analyte. A predominant challenge with metal–organic frameworks (MOFs) is their tendency to decompose in aqueous media [167], a particular concern given that electrochemical sensing operations often occur in such environments. The hydrolytic stability of MOFs is thus a paramount factor for their effective use in electroanalysis, as water molecules can disrupt the metal–ligand bonds, leading to the formation of metal hydroxides or oxides [168]. Moreover, it is well-established that many MOFs exhibit limited electrical conductivity, which is less than ideal for sensor applications [169]. To address this, various strategies have been explored to enhance both the electrical conductivity and stability of MOFs during electrochemical processes. With these improvements, we anticipate a corresponding increase in the sensitivity of electrochemical sensors utilizing MOF-based materials. Observations indicate that MOFs with nitrogen-containing ligands show enhanced hydrolytic stability compared to those with carboxylate-based ligands. This suggests a pathway to mitigate hydrolytic instability issues—by opting for MOFs with nitrogenous ligands. Additionally, selecting metal cations with higher oxidation states for the nodes and employing stable organic linkers can lead to the development of chemically robust MOFs, capable of maintaining their integrity in challenging conditions [170].

2.4.3. Biosensing

MOF-based biosensors are at the forefront of contemporary analytical science, with extensive research dedicated to the detection of a broad range of analytes [171]. The inherent structural functionality of MOFs—owing to the presence of groups such as -NH₂ or -COOH within their linkers—facilitates critical interactions like p-p stacking, hydrogen bonding, and electrostatic forces with probe biomolecules. This makes MOFs an exceptional substrate for biosensing applications. The emerging class of bimetallic MOFs is garnering attention in electrochemical biosensing due to their enhanced catalytic activities. For instance, the bimetallic ZrHf-MOFs/carbon dots composite developed by Gu et al. [172] demonstrated exceptional sensing performance for HER-2 cells, underscoring the potential of combining diverse metal elements to introduce new functionalities and achieve synergistic effects that boost the biocatalytic properties of MOFs. Figure 5 shows the different activities of typical MOFs explored as nanomasses [152].

However, despite groundbreaking developments and impressive research outputs, the field of MOF-based biosensors is still nascent, and several challenges beckon resolution: (1) Synthesizing MOF-based biosensors that meet required efficiency benchmarks remains an ongoing challenge [173–176]. (2) As the majority of MOFs are synthesized using organic solvents, their stability in aqueous environments warrants thorough investigation. (3) The creation of unique MOF-based biosensors, characterized by distinctive magnetic, thermal, and electrochemical properties, is still an objective to be realized [177–180]. (4) While MOFs can function as independent catalysts, their activity levels are generally lower than natural enzymes, likely due to the intrinsic reactivity limitations of pristine MOFs. This disparity

signifies the urgent need to design new MOF-based nanozymes with significantly higher activity profiles.

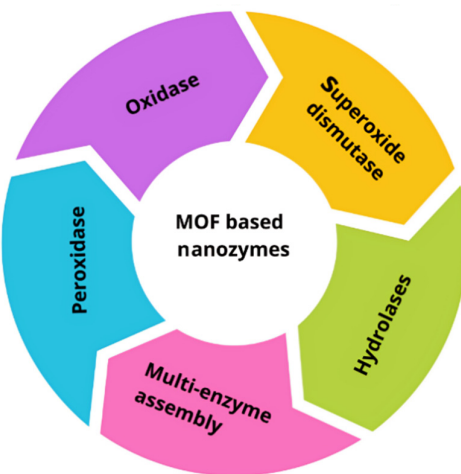


Figure 5. Typical MOFs are explored as different activities of nanozymes [152].

3. Large-Scale Preparation of MOF

Despite notable advancements in the synthesis and application of MOFs, a key concern revolves around their potential for industrialization and practical applications, particularly in high-volume use cases such as water treatment in environmental applications. Over time, the concerted efforts of material scientists and chemical engineers have optimized the synthesis of functional MOFs, making it more facile and cost-effective [46]. A range of large-scale preparation methods has been developed and considered, encompassing traditional approaches like electrochemical [24], microwave [25] and mechanochemistry [26] approaches and more recent routes like the spray dryer [27], flow chemistry [28] and high-pressure homogenization (HPH) [29]. Within this array of methods, two newly investigated approaches are delineated in the following section.

3.1. Spray-Drying (SD)

The spray drying (SD) process has been a cornerstone in industrial manufacturing for a myriad of sectors for many years [181–184]. This technique involves the atomization of a liquid or slurry into a hot gas to rapidly produce dispersed powder particles, as depicted in Figure 6. SD stands out for its ability to facilitate rapid, continuous, and scalable production of dry microspherical powders through a single-step process. The result is a reduction in fabrication costs and production times when compared to more conventional powder production methods. Since 2013, pioneering work by Arnaud Carne-Sánchez and colleagues has broadened the array of chemical processes achievable within aerosol droplets, extending beyond simple precipitation to sophisticated coordination and covalent chemistries [27]. Their research has showcased spray drying as a viable and efficient technique for the synthesis of crystalline, porous, nanostructured materials. This includes not only MOFs but also Covalent Organic Frameworks (COFs) and a variety of their composites, offering a versatile platform for material development [185]. Table 5 summarizes the common MOFs produced by spray drying with different feeding methods. The reason for choosing different methods is because before the atomization step, the precursor feed is introduced into the nozzle via simple peristaltic-pump tubing. This direct injection strategy is straightforward and convenient for precursor solutions that do not undergo any undesired reactions before spray drying. However, some precursor solutions are unstable because they contain highly reactive reagents. In these cases, the precursor solutions must first be mixed shortly before or immediately after atomization, which can be achieved through different introduction methods.

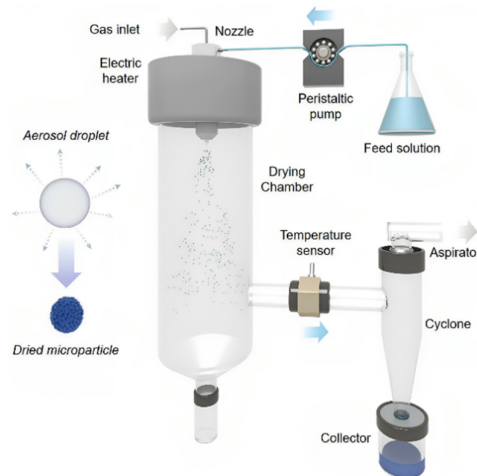


Figure 6. Schematic of the general spray drying setup [27].

Table 5. Summary of MOF and coordination polymer synthesized by spray drying.

Catalysts	Precursors	Solvent(s)	T _{inlet} (T _{coil}) [°C]	Yield [%]	S _{BET} [m ² /g]	References
HKUST-1	Cu(NO ₃) ₂ , BTC	DMF/EtOH/H ₂ O	180	70	1260	[27]
Cu-BDC	Cu(NO ₃) ₂ , BDC	DMF	180	70	543	[27]
NOTT-100	Cu(NO ₃) ₂ , BPTC	DMF/H ₂ O	180	54	1140	[27]
MOF-14	Cu(NO ₃) ₂ , BTB	DMF/EtOH/H ₂ O	180	30	-	[27]
Zn-MOF-74	Zn(NO ₃) ₂ , DHBDC	DMF/H ₂ O	180	50	-	[27]
Mg-MOF-74	Mg(NO ₃) ₂ , DHBDC	DMF/EtOH/H ₂ O	180	35	-	[27]
Ni-MOF-74	Ni(NO ₃) ₂ , DHBDC	DMF/EtOH/H ₂ O	180	40	-	[27]
MIL-88B	FeCl ₃ , NH ₂ -BDC	DMF/MeOH/H ₂ O	180	27	-	[27]
ZIF-8 ^a	Zn(OAc) ₂ , 2-MIM	H ₂ O	180	-	1634	[186]
ZIF-67 ^a	Co(OAc) ₂ , 2-MIM	H ₂ O	180	-	1861	[186]
Zn/Co-ZIF ^a	Zn(OAc) ₂ , Co(OAc) ₂ , 2-MIM	H ₂ O	180	-	1746	[186]
[Fe(NH ₂ trz) ₃]Br ₂ ·nH ₂ O	FeBr ₂ , NH ₂ -TRZ		90	-	-	[187]
[Fe(NH ₂ trz) ₃](BF ₄) _n	FeBr ₂ , NH ₂ -TRZ	EtOH; H ₂ O	90	-	-	[187]
[Fe(Htrz) ₂ (trz)](BF ₄) _n	Fe(BF ₄) ₂ , HTRZ	EtOH; H ₂ O	90	-	-	[187]
Tb0.914Eu0.086-PDA	Tb(NO ₃) ₃ , Eu(NO ₃) ₃ , PDA	DMF/H ₂ O	180	55	-	[188]
MIL-88A	FeCl ₃ , FUM	DMF/MeOH/H ₂ O	180	40	-	[27]
MOF-5	Zn(OAc) ₂ , BDC	DMF	180	60	1215	[27]
IRMOF-3	Zn(OAc) ₂ , NH ₂ -BDC	DMF	180	70	-	[27]
ZIF-8	Zn(OAc) ₂ , 2-MIM	H ₂ O	180	10	941	[27]
Cu-PB	Cu(NO ₃) ₂ , K ₃ Co(CN) ₆	H ₂ O	180	20	617	[27]
SIFSIX-3-Co	CoSiF ₆ , PYZ	MeOH	85	44	-	[189]
SIFSIX-3-Ni	NiSiF ₆ , PYZ	MeOH	85	-	-	[189]
SIFSIX-3-Cu	CuSiF ₆ , PYZ	MeOH	85	55	-	[189]
SIFSIX-3-Zn	ZnSiF ₆ , PYZ	MeOH	85	57	-	[189]
SIFSIX-1-Zn	ZnSiF ₆ , BPY	MeOH	85	40	-	[189]
TIFSIX-1-Cu	Cu(NO ₃) ₂ , BPY	MeOH	130	79	-	[189]
UiO-66	ZrCl ₄ , BDC	DMF/H ₂ O	180 (115)	70	1106	[190]
UiO-66-NH ₂	ZrCl ₄ , NH ₂ -BDC	DMF/H ₂ O	180 (115)	67	752	[190]
UiO-66-NO ₂	ZrCl ₄ , NO ₂ -BDC	acetic acid/H ₂ O	180 (115)	62	679	[190]
UiO-66-Br	ZrCl ₄ , Br-BDC	DMF/H ₂ O	180 (115)	68	527	[190]
UiO-66-(OH) ₂	ZrCl ₄ , (OH) ₂ -BDC	DMF/H ₂ O	180 (115)	81	401	[190]
UiO-66-acetamido	ZrCl ₄ , acetamido-BDC	DMF/H ₂ O	180 (115)	51	586	[190]
UiO-66-1,4-NDC	ZrCl ₄ , 1,4-NDC	DMF/H ₂ O	180 (115)	45	431	[190]
UiO-66-2,6-NDC	ZrCl ₄ , 2,6-NDC	DMF/H ₂ O	180 (115)	49	557	[190]
Fe-BTC/MIL-100	Fe(NO ₃) ₃ , BTC	DMF	180 (135)	78	1039	[190]
Ni ₈ (OH) ₄ (H ₂ O) ₂ (L) ₆	Ni(OAc) ₂ , PCA	DMF/H ₂ O	180 (100)	60	377	[190]
UiO-66-NH ₂	ZrOCl ₂ , NH ₂ -BDC	acetic acid/H ₂ O	150 (90)	64	1261	[191]
Zr-fumarate	ZrOCl ₂ , FUM	acetic acid/H ₂ O	140 (90)	58	664	[191]

Crystallized in a solvent after spray drying. BTC, trimesic acid; BDC, terephthalic acid; BPTC, biphenyl-3,3',5,5'-tetracarboxylic acid; BTB, 1,3,5-tris(4-carboxyphenylbenzene); DHBDC, 2,5-dihydroxy-terephthalic acid; 2-MIM, 2-methylimidazole; R-TRZ, 4-R-substituted-1,2,4-triazole; PDA, 1,4-phenylenediacetic acid; FUM, fumaric acid; PYZ, pyrazine; BPY, 4,4'-bipyridine; NDC, naphthalenedicarboxylic acid; PCA, 1H-pyrazole-4-carboxylic acid.

In the synthesis of MOFs via spray drying, critical parameters that require meticulous management include (1) the feed rate, which determines the amount of liquid precursor introduced into the drying system; (2) the atomization flow rate, affecting the size of liquid droplets formed; (3) the inlet temperature (T_{inlet}), which is pivotal for drying the aerosol droplets efficiently; and (4) for continuous flow-assisted synthesis, the coil-flow reactor temperature (T_{coil}) needs careful adjustment. Researchers are tasked with striking an optimal balance among these factors. For example, an increased feed rate can boost production; however, it necessitates greater energy input for atomization and drying, thus raising operational costs [27,185,192–194].

It is evident that obtaining optimal conditions for producing specific MOFs requires experimental methods based on real and reliable data and phenomena. However, due to limitations in experimental technology, equipment, measurement methods, and other factors, experimental costs are high, cycles are long, and data fluctuations are significant. The spray drying tower, during the experiment, is relatively closed and is considered a “black box”. The phenomena in the tower are challenging to observe, and obtaining specific information about its flow field is difficult [195,196]. In recent years, the computer hardware configuration has been constantly upgraded, and various hydrodynamic calculation models have been constantly improved. Numerical simulation provides a new way for in-depth research on hydrodynamics in spray drying towers, which is expected to solve the above problems. Therefore, relevant research on numerical simulation of MOF spray drying production needs to be promoted as soon as possible, which plays an important role in optimizing spray drying process to prepare MOFs in the long run.

3.2. High-Pressure Homogenization (HPH)

High-pressure homogenization (HPH) technology is an established method widely utilized across various industries, including biological, pharmaceutical [197], food [198–201], chemical [202], and industrial polymer synthesis [203]. It is commercially viable, cost-efficient, and straightforward to operate at room temperature. It is characterized by low energy requirements, high production efficiency, and the capacity for continuous operation [204]. In the realm of HPH, reactants are efficiently dispersed within a solvent, significantly outperforming conventional methods such as mechanochemical synthesis or twin-screw extrusion in terms of mass and thermal transfer. The technology also supports the continuous synthesis process through the sequential injection of reactants, which is a stark contrast to traditional batch methods like hydrothermal/solvothermal, sonochemical, and microwave-assisted synthesis [29,205].

Liu et al. [29] have further innovated within this space, pioneering a novel HPH-based technique for the large-scale, continuous synthesis of crystalline porous materials. The effectiveness of HPH approach in synthesizing these crystalline porous materials can be attributed to the following reasons: (1) the homogenization process induces cavitation within the pipes, potentially creating a local vacuum that protects organic ligands from partial oxidation and thereby enhances the reaction [204]; (2) the solvent environment under HPH conditions is optimized for reactant mass transfer, thereby improving the yield and consistency of the resulting products [206,207]; (3) the intense mechanical forces—shear stress, collision, high-frequency shock, and turbulent flow—induced by HPH significantly accelerate the formation of structures such as Covalent Organic Frameworks (COFs), MOFs, and Porous Organic Cages (POCs); (4) this method promises bulk production of these materials through consecutive reactant injections [208] (Figure 7). Therefore, HPH technology addresses the limitations of conventional and other reported synthesis methods by increasing yield and efficiency while reducing energy consumption and simplifying the production process. It also alleviates issues seen with mechanochemical and twin-screw extruder approaches, such as low crystallinity, inadequate mass/thermal transfer, limited reproducibility, and batch production constraints.

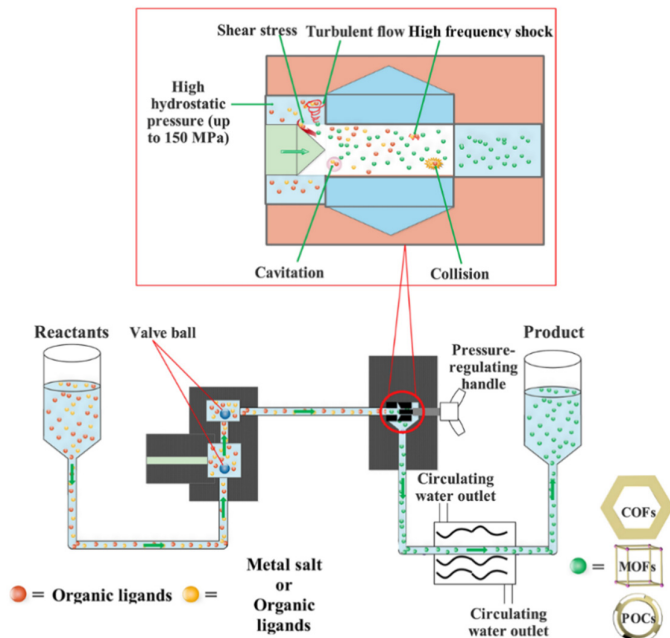


Figure 7. High pressure homogenization strategy for synthesizing crystalline porous materials [29].

Despite the advancements in mass production techniques, the synthesis of new metal-organic frameworks (MOFs) remains largely limited to certain types, hindering the diversity and innovation within this field. This bottleneck in production technology underscores a crucial need for the development of more versatile and robust mass production methods. Such advancements would not only broaden the spectrum of MOF types that can be synthesized on a commercial scale but also streamline the integration of these materials into various applications. There is a clear anticipation within the industry and academia for innovative manufacturing processes that can match the complexity of MOF chemistry with the practicalities of commercialization, thereby unlocking the full potential of MOFs in commercial applications.

4. Summary and Prospect

In summary, this discussion outlines prevailing MOF-based approaches applied in wastewater treatment to date, alongside two developed methods for large-scale MOF preparation. The significant impact of MOFs in this domain is rooted in four key attributes: (1) Enhanced stability: select MOFs maintain their integrity under a wide pH range, underscoring their viability in diverse environmental contexts. (2) Versatile ligand modifications: the adaptability in customizing MOFs through various functionalization techniques enables the integration of functional groups, enhancing the MOFs' performance. (3) Functional metal sites: the incorporation of coordinatively unsaturated metal sites within MOFs performs a dual role, anchoring pollutants for removal and serving as catalytic centers for their breakdown. (4) Multifaceted functionalization: employing a range of functionalization strategies harnesses their collective strengths, bolstering the efficiency of the pollutant degradation process.

Despite these promising features, widespread adoption of MOFs is hampered by challenges related to the materials' inherent properties and the need for better process flows. To pave the way for the wider practical application of MOFs, we present several strategic considerations: (1) Preliminary design and theoretical prediction: engage in rigorous initial design and leverage theoretical models to guide efficient large-scale synthesis. (2) Selection of organic linkers: opt for biocompatible, bio-inspired, and biodegradable organic linkers to enhance the environmental compatibility of metal-organic frameworks (MOFs). (3) Choice of reaction medium: prioritize water or green solvent systems to align with sustainable manufacturing practices. (4) Minimization of bulk organic solvents: minimize the use

of organic solvents to support eco-friendly MOF production methods. Additionally, the synthesis, reuse, and regeneration of MOFs must be considered holistically, incorporating techniques such as thermal and vacuum treatments, solvent exchange, supercritical CO₂ activation, freeze drying, and chemical activation. It is essential to establish robust protocols for recycling, regeneration, and the management of MOF waste, extending their utility across a broader spectrum of applications. A critical examination of solvent roles and choices in synthesis is paramount to forging effective, sustainable strategies for MOF production and application.

Author Contributions: Literature search, writing, and creation of figures and tables, Y.X.; review, editing and supervision, T.Z., B.W. and W.W. All authors have read and agreed to the published version of the manuscript.

Funding: This research was funded by National Natural Science Foundation of China, Grant No. 22102008.

Data Availability Statement: Not applicable.

Conflicts of Interest: The authors declare no conflicts of interest.

References

1. Liu, K.; Li, Q.; Andrade, A.L.; Wang, X.; He, Y.; Li, D. Underestimated activity-based microplastic intake under scenario-specific exposures. *Environ. Sci. Ecotechnol.* **2024**, *18*, 100316. [[CrossRef](#)] [[PubMed](#)]
2. Kutil, Z.; Novotna, K.; Cermakova, L.; Pivokonsky, M. Tunnel vision in the drinking water research field—Time for non-targeted analysis implementation? *Sci. Total Environ.* **2024**, *908*, 168367. [[CrossRef](#)] [[PubMed](#)]
3. Hou, K.; Gu, H.; Yang, Y.; Lam, S.S.; Li, H.; Sonne, C.; Ouyang, H.; Chen, X. Recent progress in advanced covalent organic framework composites for environmental remediation. *Adv. Compos. Hybrid Mater.* **2023**, *6*, 199. [[CrossRef](#)]
4. Guo, Z.; Yang, J.; Li, K.; Shi, J.; Peng, Y.; Sarkodie, E.K.; Miao, B.; Liu, H.; Liu, X.; Jiang, L. Leaching Behavior of As and Pb in Lead-Zinc Mining Waste Rock under Mine Drainage and Rainwater. *Toxics* **2023**, *11*, 943. [[CrossRef](#)] [[PubMed](#)]
5. Chaudhary, P.; Xu, M.; Ahamad, L.; Chaudhary, A.; Kumar, G.; Adeleke, B.S.; Verma, K.K.; Hu, D.M.; Širić, I.; Kumar, P.; et al. Application of Synthetic Consortia for Improvement of Soil Fertility, Pollution Remediation, and Agricultural Productivity: A Review. *Agronomy* **2023**, *13*, 643. [[CrossRef](#)]
6. Wang, B.; Lan, J.; Bo, C.; Gong, B.; Ou, J. Adsorption of heavy metal onto biomass-derived activated carbon: Review. *RSC Adv.* **2023**, *13*, 4275–4302. [[CrossRef](#)] [[PubMed](#)]
7. Kulsum, P.; Khanam, R.; Das, S.; Nayak, A.K.; Tack, F.M.; Meers, E.; Vithanage, M.; Shahid, M.; Kumar, A.; Chakraborty, S.; et al. A state-of-the-art review on cadmium uptake, toxicity, and tolerance in rice: From physiological response to remediation process. *Environ. Res.* **2023**, *220*, 115098. [[CrossRef](#)]
8. Wu, X.; Cobbina, S.J.; Mao, G.; Xu, H.; Zhang, Z.; Yang, L. A review of toxicity and mechanisms of individual and mixtures of heavy metals in the environment. *Environ. Sci. Pollut. Res.* **2016**, *23*, 8244–8259. [[CrossRef](#)] [[PubMed](#)]
9. Liu, X.; Shan, Y.; Zhang, S.; Kong, Q.; Pang, H. Application of metal organic framework in wastewater treatment. *Green Energy Environ.* **2023**, *8*, 698–721. [[CrossRef](#)]
10. Wang, C.; Liu, X.; Yang, T.; Sridhar, D.; Algadi, H.; Xu, B.B.; El-Bahy, Z.M.; Li, H.; Ma, Y.; Li, T.; et al. An overview of metal-organic frameworks and their magnetic composites for the removal of pollutants. *Sep. Purif. Technol.* **2023**, *320*, 124144. [[CrossRef](#)]
11. Qi, M.; Lin, P.; Shi, Q.; Bai, H.; Zhang, H.; Zhu, W. A metal-organic framework (MOF) and graphene oxide (GO) based peroxymonosulfate (PMS) activator applied in pollutant removal. *Process Saf. Environ. Prot.* **2023**, *171*, 847–858. [[CrossRef](#)]
12. Chang, Z.; Yang, D.H.; Xu, J.; Hu, T.L.; Bu, X.H. Flexible Metal–Organic Frameworks: Recent Advances and Potential Applications. *Adv. Mater.* **2015**, *27*, 5432–5441. [[CrossRef](#)]
13. DeCoste, J.B.; Peterson, G.W. Metal–Organic Frameworks for Air Purification of Toxic Chemicals. *Chem. Rev.* **2014**, *114*, 5695–5727. [[CrossRef](#)] [[PubMed](#)]
14. Abney, C.; Gilhula, J.; Lu, K.; Lin, W. Metal–Organic Framework Templated Inorganic Sorbents for Rapid and Efficient Extraction of Heavy Metals. *Adv. Mater.* **2014**, *26*, 7993–7997. [[CrossRef](#)] [[PubMed](#)]
15. Shao, Z.; Chen, J.; Xie, Q.; Mi, L. Functional metal/covalent organic framework materials for triboelectric nanogenerator. *Coord. Chem. Rev.* **2023**, *486*, 215118. [[CrossRef](#)]
16. Xiao, J.D.; Li, R.; Jiang, H.L. Metal–Organic Framework-Based Photocatalysis for Solar Fuel Production. *Small Methods* **2023**, *7*, 2201258. [[CrossRef](#)] [[PubMed](#)]
17. Wang, F.X.; Zhang, Z.W.; Wang, F.; Li, Y.; Zhang, Z.C.; Wang, C.C.; Yu, B.; Du, X.; Wang, P.; Fu, H.; et al. Fe–Cu bimetal metal–organic framework for efficient decontamination via Fenton-like process: Synthesis, performance and mechanism. *J. Colloid Interface Sci.* **2023**, *649*, 384–393. [[CrossRef](#)]

18. Rabeie, B.; Mahmoodi, N.M. Heterogeneous MIL-88A on MIL-88B hybrid: A promising eco-friendly hybrid from green synthesis to dual application (Adsorption and photocatalysis) in tetracycline and dyes removal. *J. Colloid Interface Sci.* **2024**, *654*, 495–522. [[CrossRef](#)] [[PubMed](#)]
19. Channab, B.E.; El Ouardi, M.; Layachi, O.A.; Marrane, S.E.; El Idrissi, A.; Baqais, A.A.; Ahsaine, H.A. Recent trends on MIL-Fe metal-organic frameworks: Synthesis approaches, structural insights, and applications in organic pollutant adsorption and photocatalytic degradation. *Environ. Sci. Nano* **2023**, *11*, 2957–2988. [[CrossRef](#)]
20. Zhu, W.; Han, M.; Kim, D.; Park, J.; Choi, H.; Kwon, G.; You, J.; Li, S.; Park, T.; Kim, J. Highly catalytic and durable nanocellulose fibers-based nanoporous membrane film for efficient organic pollutant degradation. *J. Water Process Eng.* **2023**, *53*, 103620. [[CrossRef](#)]
21. Bétard, A.; Fischer, R.A. Metal–Organic Framework Thin Films: From Fundamentals to Applications. *Chem. Rev.* **2011**, *111*, 1055–1083. [[CrossRef](#)] [[PubMed](#)]
22. Kadhom, M.; Deng, B. Metal-organic frameworks (MOFs) in water filtration membranes for desalination and other applications. *Appl. Mater. Today* **2018**, *11*, 219–230. [[CrossRef](#)]
23. Li, J.; Wang, H.; Yuan, X.; Zhang, J.; Chew, J.W. Metal-organic framework membranes for wastewater treatment and water regeneration. *Coord. Chem. Rev.* **2020**, *404*, 213116. [[CrossRef](#)]
24. Mueller, U.; Schubert, M.; Teich, F.; Puetter, H.; Schierle-Arndt, K.; Pastre, J. Metal–organic frameworks—Prospective industrial applications. *J. Mater. Chem.* **2006**, *16*, 626–636. [[CrossRef](#)]
25. Bilecka, I.; Niederberger, M. Microwave chemistry for inorganic nanomaterials synthesis. *Nanoscale* **2010**, *2*, 1358–1374. [[CrossRef](#)]
26. Kaupp, G. Solid-state molecular syntheses: Complete reactions without auxiliaries based on the new solid-state mechanism. *CrystEngComm* **2003**, *5*, 117–133. [[CrossRef](#)]
27. Carne-Sánchez, A.; Imaz, I.; Cano-Sarabia, M.; Maspoch, D. A spray-drying strategy for synthesis of nanoscale metal-organic frameworks and their assembly into hollow superstructures. *Nat. Chem.* **2013**, *5*, 203–211. [[CrossRef](#)]
28. Faustini, M.; Kim, J.; Jeong, G.Y.; Kim, J.Y.; Moon, H.R.; Ahn, W.S.; Kim, D.P. Microfluidic Approach toward Continuous and Ultrafast Synthesis of Metal–Organic Framework Crystals and Hetero Structures in Confined Microdroplets. *J. Am. Chem. Soc.* **2013**, *135*, 14619–14626. [[CrossRef](#)]
29. Liu, X.; Wang, A.; Wang, C.; Li, J.; Zhang, Z.; Al-Enizi, A.M.; Nafady, A.; Shui, F.; You, Z.; Li, B. A general large-scale synthesis approach for crystalline porous materials. *Nat. Commun.* **2023**, *14*, 7022. [[CrossRef](#)]
30. Hegde, V.; Uthappa, U.; Sunetha, M.; Altalhi, T.; Han, S.S.; Kurkuri, M.D. Functional porous Ce-Uio-66 MOF@Keratin composites for the efficient adsorption of trypan blue dye from wastewater: A step towards practical implementations. *Chem. Eng. J.* **2023**, *461*, 142103. [[CrossRef](#)]
31. Chen, J.Q.; Sharifzadeh, Z.; Bigdeli, F.; Gholizadeh, S.; Li, Z.; Hu, M.L.; Morsali, A. MOF composites as high potential materials for hazardous organic contaminants removal in aqueous environments. *J. Environ. Chem. Eng.* **2023**, *11*, 109469. [[CrossRef](#)]
32. Saglam, S.; Türk, F.N.; Arslanoglu, H. Use and applications of metal-organic frameworks (MOF) in dye adsorption: Review. *J. Environ. Chem. Eng.* **2023**, *11*, 110568. [[CrossRef](#)]
33. Crini, G.; Lichtfouse, E.; Wilson, L.D.; Morin-Crini, N. Conventional and non-conventional adsorbents for wastewater treatment. *Environ. Chem. Lett.* **2018**, *17*, 195–213. [[CrossRef](#)]
34. Lv, Z.; Fan, Q.; Xie, Y.; Chen, Z.; Alsaedi, A.; Hayat, T.; Wang, X.; Chen, C. MOFs-derived magnetic chestnut shell-like hollow sphere NiO/Ni@C composites and their removal performance for arsenic(V). *Chem. Eng. J.* **2019**, *362*, 413–421. [[CrossRef](#)]
35. Hasan, Z.; Jhung, S.H. Removal of hazardous organics from water using metal-organic frameworks (MOFs): Plausible mechanisms for selective adsorptions. *J. Hazard. Mater.* **2015**, *283*, 329–339. [[CrossRef](#)] [[PubMed](#)]
36. Tian, C.; Zhao, J.; Ou, X.; Wan, J.; Cai, Y.; Lin, Z.; Dang, Z.; Xing, B. Enhanced Adsorption of p-Arsanilic Acid from Water by Amine-Modified UiO-67 as Examined Using Extended X-ray Absorption Fine Structure, X-ray Photoelectron Spectroscopy, and Density Functional Theory Calculations. *Environ. Sci. Technol.* **2018**, *52*, 3466–3475. [[CrossRef](#)] [[PubMed](#)]
37. Shen, Y.; Tong, Y.; Xu, J.; Wang, S.; Wang, J.; Zeng, T.; He, Z.; Yang, W.; Song, S. Ni-based layered metal-organic frameworks with palladium for electrochemical dechlorination. *Appl. Catal. B Environ.* **2020**, *264*, 118505. [[CrossRef](#)]
38. Zhao, Y.; Zhao, H.; Zhao, X.; Qu, Y.; Liu, D. Synergistic effect of electrostatic and coordination interactions for adsorption removal of cephalexin from water using a zirconium-based metal-organic framework. *J. Colloid Interface Sci.* **2020**, *580*, 256–263. [[CrossRef](#)] [[PubMed](#)]
39. Zhou, W.; Dai, Q.Z.; Zhan, T.T.; Wang, L.; Bian, X.Z.; Fan, S.Q.; Xiong, P.; Xia, Y.; Chen, J.M. Adsorption removal of pharmaceutical and personal care products with functionalized metal-organic framework: Adsorptive selectivity and mechanism. *Desalination Water Treat.* **2020**, *191*, 231–238. [[CrossRef](#)]
40. Ahmed, I.; Hasan, Z.; Lee, G.; Lee, H.J.; Jhung, S.H. Contribution of hydrogen bonding to liquid-phase adsorptive removal of hazardous organics with metal-organic framework-based materials. *Chem. Eng. J.* **2022**, *430*, 132596. [[CrossRef](#)]
41. Bai, Y.; Dou, Y.; Xie, L.H.; Rutledge, W.; Li, J.R.; Zhou, H.C. Zr-based metal-organic frameworks: Design, synthesis, structure, and applications. *Chem. Soc. Rev.* **2016**, *45*, 2327–2367. [[CrossRef](#)] [[PubMed](#)]
42. Lacalamita, D.; Hoyez, G.; Mongioví, C.; Ponchel, A.; Morin-Crini, N.; Rousseau, C.; Loup, C.; Rousseau, J.; Raschetti, M.; Monflier, E. Efficient removal of fluoride ions present in industrial effluents using metal-organic frameworks of UiO-66-NH₂. *J. Water Process Eng.* **2023**, *53*, 103791. [[CrossRef](#)]

43. Keshta, B.E.; Yu, H.; Wang, L. MIL series-based MOFs as effective adsorbents for removing hazardous organic pollutants from water. *Sep. Purif. Technol.* **2023**, *322*, 124301. [[CrossRef](#)]
44. Batra, R.; Chen, C.; Evans, T.G.; Walton, K.S.; Ramprasad, R. Prediction of water stability of metal–organic frameworks using machine learning. *Nat. Mach. Intell.* **2020**, *2*, 704–710. [[CrossRef](#)]
45. Yan, C.; Jin, J.; Wang, J.; Zhang, F.; Tian, Y.; Liu, C.; Zhang, F.; Cao, L.; Zhou, Y.; Han, Q. Metal–organic frameworks (MOFs) for the efficient removal of contaminants from water: Underlying mechanisms, recent advances, challenges, and future prospects. *Coord. Chem. Rev.* **2022**, *468*, 214595. [[CrossRef](#)]
46. Abdi, J.; Sisi, A.J.; Hadipoor, M.; Khataee, A. State of the art on the ultrasonic-assisted removal of environmental pollutants using metal–organic frameworks. *J. Hazard. Mater.* **2022**, *424*, 127558. [[CrossRef](#)]
47. Yuan, N.; Gong, X.; Sun, W.; Yu, C. Advanced applications of Zr-based MOFs in the removal of water pollutants. *Chemosphere* **2021**, *267*, 128863. [[CrossRef](#)]
48. Zango, Z.U.; Jumbri, K.; Sambudi, N.S.; Ramli, A.; Abu Bakar, N.H.H.; Saad, B.; Rozaini, M.N.H.; Isiyaka, H.A.; Jagaba, A.H.; Aldaghri, O.; et al. A Critical Review on Metal–Organic Frameworks and Their Composites as Advanced Materials for Adsorption and Photocatalytic Degradation of Emerging Organic Pollutants from Wastewater. *Polymers* **2020**, *12*, 2648. [[CrossRef](#)]
49. Yoo, D.K.; Bhadra, B.N.; Jhung, S.H. Adsorptive removal of hazardous organics from water and fuel with functionalized metal–organic frameworks: Contribution of functional groups. *J. Hazard. Mater.* **2021**, *403*, 123655. [[CrossRef](#)]
50. Ibrahim, A.O.; Adegoke, K.A.; Adegoke, R.O.; Abdulwahab, Y.A.; Oyelami, V.B.; Adesina, M.O. Adsorptive removal of different pollutants using metal–organic framework adsorbents. *J. Mol. Liq.* **2021**, *333*, 115593. [[CrossRef](#)]
51. Nguyen, D.A.; Nguyen, D.V.; Jeong, G.; Asghar, N.; Jang, A. Critical evaluation of hybrid metal–organic framework composites for efficient treatment of arsenic-contaminated solutions by adsorption and membrane-separation process. *Chem. Eng. J.* **2023**, *461*, 141789. [[CrossRef](#)]
52. Abdelhameed, R.M.; Abdel-Gawad, H.; Elshahat, M.; Emam, H.E. Cu–BTC@cotton composite: Design and removal of ethion insecticide from water. *RSC Adv.* **2016**, *6*, 42324–42333. [[CrossRef](#)]
53. Schelling, M.; Kim, M.; Otal, E.; Hinestroza, J. Decoration of Cotton Fibers with a Water-Stable Metal–Organic Framework (UiO-66) for the Decomposition and Enhanced Adsorption of Micropollutants in Water. *Bioengineering* **2018**, *5*, 14. [[CrossRef](#)] [[PubMed](#)]
54. Dahlan, I.; Wan Mazlan, W.H.; Mulkan, A.; Zwain, H.M.; Hassan, S.R.; Aziz, H.A.; Hasan, H.Y.A.; Zekker, I. Modeling of Batch Organic Dye Adsorption Using Modified Metal–Organic Framework-5. *Chem. Eng. Technol.* **2022**, *45*, 2080–2087. [[CrossRef](#)]
55. Tran, T.K.N.; Phan, C.P.K.; Ngo, T.C.Q.; Hoang, N.B.; Truong, L.D.; Nguyen, T.K.O. Synthesis and Characterization Bimetallic Organic Framework CoxFex(BDC) and Adsorption Cationic and Anionic Dyes. *Processes* **2022**, *10*, 1352. [[CrossRef](#)]
56. Qin, Z.; Xiang, S.; Jing, Z.; Deng, M.; Jiang, W.; Yao, L.; Yang, L.; Deng, L.; Dai, Z. Thin film nanocomposite membranes fabricated via 2D ZIF-67 nanosheets and 1D nanofibers with ultrahigh water flux for dye removal from wastewater. *Sep. Purif. Technol.* **2024**, *330*, 125308. [[CrossRef](#)]
57. Cheng, B.; Fu, X.; Song, Y.; Li, Z.; Weng, P.; Yin, X. A versatile MOF liquids-based Janus fibrous membrane towards complex oil/water separation and heavy metal ions removal. *Sep. Purif. Technol.* **2024**, *331*, 125701. [[CrossRef](#)]
58. Valverde, A.; de Fernandez-de Luis, R.; Salazar, H.; Gonçalves, B.F.; King, S.; Almásy, L.; Kriegbaum, M.; Laza, J.M.; Vilas-Vilela, J.L.; Martins, P.M. On The Multiscale Structure and Morphology of Pvdf-Hfp@Mof Membranes in The Scope of Water Remediation Applications. *Adv. Mater. Interfaces* **2023**, *10*, 2300424. [[CrossRef](#)]
59. Ali, Z.; Naz, A.; Haq, N.U.; Nazir, A.; Munawar, A.; Khan, A.L.; Elqahtani, Z.M.; Alwadai, N.; Younas, U.; Iqbal, M. Fabrication of novel Zn (II)-imidazole based mixed matrix membranes for heavy metal removals from drinking water. *Z. Fur Phys. Chem.* **2023**, *237*, 951–967. [[CrossRef](#)]
60. Wang, L.; Huang, J.; Li, Z.; Han, Z.; Fan, J. Review of Synthesis and Separation Application of Metal–Organic Framework-Based Mixed-Matrix Membranes. *Polymers* **2023**, *15*, 1950. [[CrossRef](#)]
61. Arjmandi, M.; Peyravi, M.; Chenar, M.P.; Jahanshahi, M. Channelization of water pathway and encapsulation of DS in the SL of the TFC FO membrane as a novel approach for controlling dilutive internal concentration polarization. *Environ. Sci. Water Res. Technol.* **2019**, *5*, 1436–1452. [[CrossRef](#)]
62. Liu, L.; Luo, X.B.; Ding, L.; Luo, S.L. Application of nanotechnology in the removal of heavy metal from water. In *Nanomaterials for the Removal of Pollutants and Resource Reutilization*; Luo, X.B., Deng, F., Eds.; Elsevier: Amsterdam, The Netherlands, 2019; pp. 83–147.
63. Arjmandi, M.; Pourafshari Chenar, M.; Peyravi, M.; Jahanshahi, M. Physical modification of polymeric support layer for thin film composite forward osmosis membranes by metal–organic framework-based porous matrix membrane strategy. *J. Appl. Polym. Sci.* **2020**, *137*, 48672. [[CrossRef](#)]
64. Ding, C.; Yin, J.; Deng, B. Effects of polysulfone (PSf) support layer on the performance of thin-film composite (TFC) membranes. *J. Chem. Process Eng.* **2014**, *1*, 1–8. [[CrossRef](#)]
65. Li, Q.; Li, J.; Fang, X.; Liao, Z.; Wang, D.; Sun, X.; Shen, J.; Han, W.; Wang, L. Interfacial growth of metal–organic framework membranes on porous polymers via phase transformation. *Chem. Commun.* **2018**, *54*, 3590–3593. [[CrossRef](#)]
66. Chen, X.; Han, R.; Guo, Z.; Ma, H.; Ji, X.; Wang, L.; Meng, J.; Fang, Y.; Pang, K.; Peng, S. Photocatalytic and Superhydrophobic Nanoporous Membranes for Emulsion Separation and Removal of Pesticides and Pharmaceutical Products. *ACS Appl. Nano Mater.* **2024**, *7*, 4288–4301. [[CrossRef](#)]

67. Dutta, S.; Patel, B.M.; Singh, Y.; Hegde, G.; Bose, S. Photocatalytic driven ‘self-cleaning’ IPN membranes infused with a ‘host-guest’ pair consisting of metal-organic framework encapsulated anionic ‘nano-clusters’ for water remediation. *J. Membr. Sci.* **2024**, *694*, 122422. [[CrossRef](#)]
68. Jiang, H.; Xu, M.; Leng, C.; Ma, Q.; Dai, J.; Feng, S.; Wang, N.; Wei, J.; Wang, L. Bifunctional MOF-5@ coal-based fiber membrane for oil-water separation and dye adsorption. *Colloids Surf. A Physicochem. Eng. Asp.* **2024**, *683*, 133021. [[CrossRef](#)]
69. Peng, S.; Ma, H.; Hao, X.; Han, R.; Ji, X.; Wang, L.; Fang, Y.; Pang, K.; Il-Ho, K.; Chen, X. Constructing green superhydrophilic and superoleophobic COFs-MOFs hybrid-based membrane for efficiently emulsion separation and synchronous removal of microplastics, dyes, and pesticides. *Environ. Res.* **2024**, *243*, 117777. [[CrossRef](#)]
70. Xu, H.; Chen, S.; Zhao, Y.F.; Wang, F.; Guo, F. MOF-Based Membranes for Remediated Application of Water Pollution. *ChemPlusChem* **2024**, *18*, e202400027. [[CrossRef](#)]
71. Jia, F.; Yang, L.; Sun, L.; Yu, D.; Song, Y.; Wang, Y.; Kipper, M.J.; Tang, J.; Huang, L. Efficient separation of dyes using two-dimensional heterogeneous composite membranes. *Water Res.* **2023**, *247*, 120693. [[CrossRef](#)]
72. Yang, S.; Zou, Q.; Wang, T.; Zhang, L. Effects of GO and MOF@GO on the permeation and antifouling properties of cellulose acetate ultrafiltration membrane. *J. Membr. Sci.* **2019**, *569*, 48–59. [[CrossRef](#)]
73. Hani, A.; Haikal, R.R.; El-Mehalmey, W.A.; Safwat, Y.; Alkordi, M.H. Durable and recyclable MOF@ polycaprolactone mixed-matrix membranes with hierarchical porosity for wastewater treatment. *Nanoscale* **2023**, *15*, 19617–19628. [[CrossRef](#)] [[PubMed](#)]
74. Xiang, B.; Gong, J.; Sun, Y.; Li, J. Robust PVA/GO@MOF membrane with fast photothermal self-cleaning property for oily wastewater purification. *J. Hazard. Mater.* **2024**, *462*, 132803. [[CrossRef](#)] [[PubMed](#)]
75. He, X.; Liu, X.; Liu, J.; Li, B.; Liu, H.; Tao, W.; Xu, X.; Li, Z. Self-assembled superhydrophilic MOF-decorated membrane for highly efficient treatment and separation mechanism of multi-component emulsions. *Desalination* **2024**, *569*, 117047. [[CrossRef](#)]
76. Xiang, W.; Wang, Q.; Li, Z.; Dong, J.; Liu, J.; Zhang, L.; Xia, T.; He, Y.; Zhao, D. Water-stable methyl-modified MOF and mixed matrix membrane for efficient adsorption and separation of cationic dyes. *Sep. Purif. Technol.* **2024**, *330*, 125268. [[CrossRef](#)]
77. Yang, H.; Zhang, P.; Zheng, Q.; Hameed, M.U.; Raza, S. Synthesis of cellulose cotton-based UiO-66 MOFs for the removal of rhodamine B and Pb (II) metal ions from contaminated wastewater. *Int. J. Biol. Macromol.* **2023**, *253*, 126986. [[CrossRef](#)] [[PubMed](#)]
78. Daraei, P.; Rostami, E.; Nasirmanesh, F.; Nobakht, V. Preparation of pH-sensitive composite polyethersulfone membranes embedded by Ag (I) coordination polymer for the removal of cationic and anionic dyes. *J. Environ. Manag.* **2023**, *347*, 119083. [[CrossRef](#)] [[PubMed](#)]
79. Hu, Q.H.; Tang, D.Y.; Wang, X.H.; Yan, L.L.; Deng, L.L.; Zhao, M.Q.; Deng, E.N.; Zhou, Q.H. Molecularly imprinted MOF/PAN hybrid nanofibrous membranes for selective bisphenol A adsorption and antibacterial fouling in water treatment. *Sep. Purif. Technol.* **2024**, *328*, 124984. [[CrossRef](#)]
80. Mukherjee, D.; Pal, S.C.; Das, G.; Gore, K.R.; Das, M.C. Devising robust hydrophobic MOFs and its membrane for ultra-sensitive aqueous phase detection of antibiotics and toxic nitro-explosives and adsorption of TNP. *J. Environ. Chem. Eng.* **2023**, *11*, 110528. [[CrossRef](#)]
81. Wang, J.; Wang, S. Activation of persulfate (PS) and peroxymonosulfate (PMS) and application for the degradation of emerging contaminants. *Chem. Eng. J.* **2018**, *334*, 1502–1517. [[CrossRef](#)]
82. Mojiri, A.; Zhou, J.L.; Ozaki, N.; Karimidermani, B.; Razmi, E.; Kasmuri, N. Occurrence of per- and polyfluoroalkyl substances in aquatic environments and their removal by advanced oxidation processes. *Chemosphere* **2023**, *330*, 138666. [[CrossRef](#)] [[PubMed](#)]
83. Hu, X.; Bao, J.; Chen, D.; Shah, S.J.; Subhan, S.; Gong, W.; Li, W.; Luan, X.; Zhao, Z.; Zhao, Z. Accelerating the Fe(III)/Fe(II) cycle via enhanced electronic effect in NH₂-MIL-88B(Fe)/TPB-DMTP-COF composite for boosting photo-Fenton degradation of sulfamerazine. *J. Colloid Interface Sci.* **2022**, *624*, 121–136. [[CrossRef](#)] [[PubMed](#)]
84. Wang, F.X.; Wang, C.C.; Du, X.; Li, Y.; Wang, F.; Wang, P. Efficient removal of emerging organic contaminants via photo-Fenton process over micron-sized Fe-MOF sheet. *Chem. Eng. J.* **2022**, *429*, 132495. [[CrossRef](#)]
85. Wenderich, K.; Mul, G. Methods, Mechanism, and Applications of Photodeposition in Photocatalysis: A Review. *Chem. Rev.* **2016**, *116*, 14587–14619. [[CrossRef](#)] [[PubMed](#)]
86. Babuponnusami, A.; Muthukumar, K. A review on Fenton and improvements to the Fenton process for wastewater treatment. *J. Environ. Chem. Eng.* **2014**, *2*, 557–572. [[CrossRef](#)]
87. Du, X.; Oturan, M.A.; Zhou, M.; Belkessa, N.; Su, P.; Cai, J.; Trellu, C.; Mousset, E. Nanostructured electrodes for electrocatalytic advanced oxidation processes: From materials preparation to mechanisms understanding and wastewater treatment applications. *Appl. Catal. B Environ.* **2021**, *296*, 120332. [[CrossRef](#)]
88. von Gunten, U. Ozonation of drinking water: Part I. Oxidation kinetics and product formation. *Water Res.* **2003**, *37*, 1443–1467. [[CrossRef](#)] [[PubMed](#)]
89. Thomas, N.; Dionysiou, D.D.; Pillai, S.C. Heterogeneous Fenton catalysts: A review of recent advances. *J. Hazard. Mater.* **2021**, *404*, 124082. [[CrossRef](#)] [[PubMed](#)]
90. Feng, C.; Liu, S.; Tan, X.; Dai, M.; Chen, Q.; Huang, X. Polydopamine-modified MOF-5-derived carbon as persulfate activator for aniline aerofloat degradation. *Chemosphere* **2023**, *345*, 140436. [[CrossRef](#)]
91. Wu, S.; Zhao, M.; Xia, Z.; Liu, J.; Chen, Y.; Lv, X.; Jia, Z.; Xie, Z. Highly dispersed Co on N-doped carbon derived from metal-organic framework composite for enhanced peroxymonosulfate activation toward tetracycline degradation. *Diam. Relat. Mater.* **2023**, *140*, 110544. [[CrossRef](#)]

92. Liu, J.; Zhao, L.; Geng, H.; Wang, B.; Tong, X.; Li, Y.; Chen, D.; Sun, P.; Yang, Y. Fe-MOF-derived carbon compounds as catalysts for trichloroethylene degradation via persulfate oxidation: Role of precursor template and pyrolysis temperature. *J. Environ. Chem. Eng.* **2023**, *11*, 110649. [[CrossRef](#)]
93. Wang, Q.; Lu, J.; Jiang, Y.; Yang, S.; Yang, Y.; Wang, Z. FeCo bimetallic metal organic framework nanosheets as peroxyomonosulfate activator for selective oxidation of organic pollutants. *Chem. Eng. J.* **2022**, *443*, 136483. [[CrossRef](#)]
94. Ren, Y.; Wang, S.; Zhang, J.; Lu, J.; Shan, C.; Zhang, Y.; Dionysiou, D.D.; Lv, L.; Pan, B.; Zhang, W. Enhancing the performance of Fenton-like oxidation by a dual-layer membrane: A sequential interception-oxidation process. *J. Hazard. Mater.* **2021**, *402*, 123766. [[CrossRef](#)] [[PubMed](#)]
95. Araya, T.; Jia, M.; Yang, J.; Zhao, P.; Cai, K.; Ma, W.; Huang, Y. Resin modified MIL-53 (Fe) MOF for improvement of photocatalytic performance. *Appl. Catal. B Environ.* **2017**, *203*, 768–777. [[CrossRef](#)]
96. Araya, T.; Chen, C.C.; Jia, M.K.; Johnson, D.; Li, R.; Huang, Y.P. Selective degradation of organic dyes by a resin modified Fe-based metal-organic framework under visible light irradiation. *Opt. Mater.* **2017**, *64*, 512–523. [[CrossRef](#)]
97. Tang, M.; Wan, J.; Wang, Y.; Yan, Z.; Ma, Y.; Sun, J.; Ding, S. Developing a molecularly imprinted channels catalyst based on template effect for targeted removal of organic micropollutants from wastewaters. *Chem. Eng. J.* **2022**, *445*, 136755. [[CrossRef](#)]
98. Ding, S.; Wan, J.; Ma, Y.; Wang, Y.; Li, X.; Sun, J.; Pu, M. Targeted degradation of dimethyl phthalate by activating persulfate using molecularly imprinted Fe-MOF-74. *Chemosphere* **2021**, *270*, 128620. [[CrossRef](#)] [[PubMed](#)]
99. Ding, S.; Wan, J.; Wang, Y.; Yan, Z.; Ma, Y. Activation of persulfate by molecularly imprinted Fe-MOF-74@SiO₂ for the targeted degradation of dimethyl phthalate: Effects of operating parameters and chlorine. *Chem. Eng. J.* **2021**, *422*, 130406. [[CrossRef](#)]
100. Yao, Y.; Wang, C.; Yan, X.; Zhang, H.; Xiao, C.; Qi, J.; Zhu, Z.; Zhou, Y.; Sun, X.; Duan, X.; et al. Rational Regulation of Co-N-C Coordination for High-Efficiency Generation of ¹O₂ toward Nearly 100% Selective Degradation of Organic Pollutants. *Environ. Sci. Technol.* **2022**, *56*, 8833–8843. [[CrossRef](#)]
101. Liu, Y.; Miao, W.; Feng, Y.; Fang, X.; Li, Q.; Du, N.; Wang, D.; Mao, S. Enhanced peroxydisulfate oxidation via Cu(III) species with a Cu-MOF-derived Cu nanoparticle and 3D graphene network. *J. Hazard. Mater.* **2021**, *403*, 123691. [[CrossRef](#)]
102. Liu, X.; Liu, Y.; Qin, H.; Ye, Z.; Wei, X.; Miao, W.; Yang, D.; Mao, S. Selective Removal of Phenolic Compounds by Peroxydisulfate Activation: Inherent Role of Hydrophobicity and Interface ROS. *Environ. Sci. Technol.* **2022**, *56*, 2665–2676. [[CrossRef](#)] [[PubMed](#)]
103. Schweitzer, C.; Schmidt, R. Physical Mechanisms of Generation and Deactivation of Singlet Oxygen. *Chem. Rev.* **2003**, *103*, 1685–1757. [[CrossRef](#)]
104. Mazarji, M.; Minkina, T.; Sushkova, S.; Mandzhieva, S.; Bayero, M.T.; Fedorenko, A.; Mahmoodi, N.M.; Sillanpää, M.; Bauer, T.; Soldatov, A. Metal-organic frameworks (MIL-101) decorated biochar as a highly efficient bio-based composite for immobilization of polycyclic aromatic hydrocarbons and copper in real contaminated soil. *J. Environ. Chem. Eng.* **2022**, *10*, 108821. [[CrossRef](#)]
105. Zhi, G.; Qi, X.; Li, Y.; Wang, J.; Wang, J. Efficient treatment of smelting wastewater: 3D nickel foam @MOF shatters the previous limitation, enabling high-throughput selective capture of arsenic to form non-homogeneous nuclei. *Sep. Purif. Technol.* **2024**, *328*, 124927. [[CrossRef](#)]
106. Li, X.; Zheng, S.; Li, Y.; Ding, J.; Qin, W. Effectively facilitating the degradation of chloramphenicol by the synergism of *Shewanella oneidensis* MR-1 and the metal-organic framework. *J. Hazard. Mater.* **2023**, *454*, 131545. [[CrossRef](#)]
107. Li, Y.; Xu, Z.; Wang, W.X. Effective flocculation of harmful algae *Microcystis aeruginosa* by nanoscale metal-organic framework NH2-MIL-101(Cr). *Chem. Eng. J.* **2022**, *433*, 134584. [[CrossRef](#)]
108. Wang, Z.; Xu, Y.; Wang, C.; Yue, L.; Liu, T.; Lan, Q.; Cao, X.; Xing, B. Photocatalytic inactivation of harmful algae *Microcystis aeruginosa* and degradation of microcystin by g-C₃N₄/Cu-MOF nanocomposite under visible light. *Sep. Purif. Technol.* **2023**, *313*, 123515. [[CrossRef](#)]
109. Kim, Y.; Kalimuthu, P.; Nam, G.; Jung, J. Cyanobacteria control using Cu-based metal organic frameworks derived from waste PET bottles. *Environ. Res.* **2023**, *224*, 115532. [[CrossRef](#)] [[PubMed](#)]
110. Liu, Y.; Yang, M.; Cao, Y.; Xu, M.; Zhang, H.; Zhao, W.; Wang, R.; Yang, Y.; Chen, J. Inhibition of growth for *Microcystis aeruginosa* by insertion of iron ion into biochar modified copper metal organic framework (Fe₃O₄-BC@Cu-MOF-74) under visible light. *J. Environ. Chem. Eng.* **2023**, *11*, 111130. [[CrossRef](#)]
111. Fan, G.; Zhou, J.; Zheng, X.; Chen, W. Growth Inhibition of *Microcystis aeruginosa* by Copper-based MOFs: Performance and Physiological Effect on Algal Cells. *Appl. Organomet. Chem.* **2018**, *32*, e4600. [[CrossRef](#)]
112. Vasseghian, Y.; Khaneghah, A.M.; Khataee, A. New emerging techniques for detection and degradation of hazardous materials in environments: Challenges and perspectives. *Chemosphere* **2022**, *286*, 131589. [[CrossRef](#)] [[PubMed](#)]
113. Diamantis, S.A.; Margariti, A.; Pournara, A.D.; Papaefstathiou, G.S.; Manos, M.J.; Lazarides, T. Luminescent metal-organic frameworks as chemical sensors: Common pitfalls and proposed best practices. *Inorg. Chem. Front.* **2018**, *5*, 1493–1511. [[CrossRef](#)]
114. Cui, A.Q.; Wu, X.Y.; Ye, J.B.; Song, G.; Chen, D.Y.; Xu, J.; Liu, Y.; Lai, J.P.; Sun, H. Two-in-one? dual-function luminescent MOF hydrogel for onsite ultra-sensitive detection and efficient enrichment of radioactive uranium in water. *J. Hazard. Mater.* **2023**, *448*, 130864. [[CrossRef](#)] [[PubMed](#)]
115. Yan, D.; Lou, Y.; Yang, Y.; Chen, Z.; Cai, Y.; Guo, Z.; Zhan, H.; Chen, B. Dye-Modified Metal-Organic Framework as a Recyclable Luminescent Sensor for Nicotine Determination in Urine Solution and Living Cell. *ACS Appl. Mater. Interfaces* **2019**, *11*, 47253–47258. [[CrossRef](#)] [[PubMed](#)]
116. Qu, S.; Li, Z.; Jia, Q. Detection of Purine Metabolite Uric Acid with Picolinic-Acid-Functionalized Metal-Organic Frameworks. *ACS Appl. Mater. Interfaces* **2019**, *11*, 34196–34202. [[CrossRef](#)] [[PubMed](#)]

117. Yu, H.; Fan, M.; Liu, Q.; Su, Z.; Li, X.; Pan, Q.; Hu, X. Two Highly Water-Stable Imidazole-Based Ln-MOFs for Sensing Fe^{3+} , $\text{Cr}_2\text{O}_7^{2-}$ /CrO $^{2-}_4$ in a Water Environment. *Inorg. Chem.* **2020**, *59*, 2005–2010. [CrossRef] [PubMed]
118. Zhang, X.; Zhang, Q.; Yue, D.; Zhang, J.; Wang, J.; Li, B.; Yang, Y.; Cui, Y.; Qian, G. Flexible Metal–Organic Framework-Based Mixed-Matrix Membranes: A New Platform for H₂S Sensors. *Small* **2018**, *14*, 1801563. [CrossRef] [PubMed]
119. Razavi, S.A.A.; Masoomi, M.Y.; Morsali, A. Morphology-dependent sensing performance of dihydro-tetrazine functionalized MOF toward Al(III). *Ultrason. Sonochem.* **2018**, *41*, 17–26. [CrossRef]
120. Sousaraei, A.; Queirós, C.; Moscoso, F.G.; Lopes-Costa, T.; Pedrosa, J.M.; Silva, A.M.; Cunha-Silva, L.; Cabanillas-Gonzalez, J. Subppm Amine Detection via Absorption and Luminescence Turn-On Caused by Ligand Exchange in Metal Organic Frameworks. *Anal. Chem.* **2019**, *91*, 15853–15859. [CrossRef]
121. Maka, V.K.; Mukhopadhyay, A.; Savitha, G.; Moorthy, J.N. Fluorescent 2D metal–organic framework nanosheets (MONs): Design, synthesis and sensing of explosive nitroaromatic compounds (NACs). *Nanoscale* **2018**, *10*, 22389–22399. [CrossRef]
122. Han, L.J.; Zheng, D.; Chen, S.G.; Zheng, H.G.; Ma, J. A Highly Solvent-Stable Metal–Organic Framework Nanosheet: Morphology Control, Exfoliation, and Luminescent Property. *Small* **2018**, *14*, 1703873. [CrossRef] [PubMed]
123. Wei, J.Z.; Wang, X.L.; Sun, X.J.; Hou, Y.; Zhang, X.; Yang, D.D.; Dong, H.; Zhang, F.M. Rapid and Large-Scale Synthesis of IRMOF-3 by Electrochemistry Method with Enhanced Fluorescence Detection Performance for TNP. *Inorg. Chem.* **2018**, *57*, 3818–3824. [CrossRef] [PubMed]
124. Yang, L.; Song, Y.; Wang, L. Multi-emission metal–organic framework composites for multicomponent ratiometric fluorescence sensing: Recent developments and future challenges. *J. Mater. Chem. B* **2020**, *8*, 3292–3315. [CrossRef] [PubMed]
125. Wu, S.; Min, H.; Shi, W.; Cheng, P. Multicenter Metal–Organic Framework-Based Ratiometric Fluorescent Sensors. *Adv. Mater.* **2019**, *32*, 1805871. [CrossRef] [PubMed]
126. Chen, L.; Liu, D.; Peng, J.; Du, Q.; He, H. Ratiometric fluorescence sensing of metal-organic frameworks: Tactics and perspectives. *Coord. Chem. Rev.* **2020**, *404*, 213113. [CrossRef]
127. Li, C.; Hai, J.; Li, S.; Wang, B.; Yang, Z. Luminescent magnetic nanoparticles encapsulated in MOFs for highly selective and sensitive detection of ClO $^-$ /SCN $^-$ and anti-counterfeiting. *Nanoscale* **2018**, *10*, 8667–8676. [CrossRef]
128. Das, P.; Mandal, S.K. Strategic Design and Functionalization of an Amine-Decorated Luminescent Metal Organic Framework for Selective Gas/Vapor Sorption and Nanomolar Sensing of 2,4,6-Trinitrophenol in Water. *ACS Appl. Mater. Interfaces* **2018**, *10*, 25360–25371. [CrossRef] [PubMed]
129. Guo, L.; Liang, M.; Wang, X.; Kong, R.; Chen, G.; Xia, L.; Qu, F. The role of l-histidine as molecular tongs: A strategy of grasping Tb $^{3+}$ using ZIF-8 to design sensors for monitoring an anthrax biomarker on-the-spot. *Chem. Sci.* **2020**, *11*, 2407–2413. [CrossRef]
130. Dalapati, R.; Biswas, S. A Pyrene-Functionalized Metal–Organic Framework for Nonenzymatic and Ratiometric Detection of Uric Acid in Biological Fluid via Conformational Change. *Inorg. Chem.* **2019**, *58*, 5654–5663. [CrossRef]
131. Pan, H.; Wang, S.; Dao, X.; Ni, Y. Fluorescent Zn-PDC/Tb $^{3+}$ Coordination Polymer Nanostructure: A Candidate for Highly Selective Detections of Cefixime Antibiotic and Acetone in Aqueous System. *Inorg. Chem.* **2018**, *57*, 1417–1425. [CrossRef]
132. Gao, X.; Zhao, H.; Zhao, X.; Li, Z.; Gao, Z.; Wang, Y.; Huang, H. Aqueous phase sensing of bismuth ion using fluorescent metal-organic framework. *Sens. Actuators B Chem.* **2018**, *266*, 323–328. [CrossRef]
133. Aswathi, R.; Sandhya, K.Y. Ultrasensitive and selective electrochemical sensing of Hg(ii) ions in normal and sea water using solvent exfoliated MoS₂: Affinity matters. *J. Mater. Chem. A* **2018**, *6*, 14602–14613. [CrossRef]
134. Sheng, S.; Zhang, Z.; Wang, M.; He, X.; Jiang, C.; Wang, Y. Synthesis of MIL-125(Ti) derived TiO₂ for selective photoelectrochemical sensing and photocatalytic degradation of tetracycline. *Electrochim. Acta* **2022**, *420*, 140441. [CrossRef]
135. Chai, X.; Zhou, X.; Zhu, A.; Zhang, L.; Qin, Y.; Shi, G.; Tian, Y. A Two-Channel Ratiometric Electrochemical Biosensor for In Vivo Monitoring of Copper Ions in a Rat Brain Using Gold Truncated Octahedral Microcages. *Angew. Chem. Int. Ed.* **2013**, *52*, 8129–8133. [CrossRef] [PubMed]
136. Xiao, L.; Xu, H.; Zhou, S.; Song, T.; Wang, H.; Li, S.; Gan, W.; Yuan, Q. Simultaneous detection of Cd(II) and Pb(II) by differential pulse anodic stripping voltammetry at a nitrogen-doped microporous carbon/Nafion/bismuth-film electrode. *Electrochim. Acta* **2014**, *143*, 143–151. [CrossRef]
137. Guo, H.; Zheng, Z.; Zhang, Y.; Lin, H.; Xu, Q. Highly selective detection of Pb $^{2+}$ by a nanoscale Ni-based metal–organic framework fabricated through one-pot hydrothermal reaction. *Sens. Actuators B Chem.* **2017**, *248*, 430–436. [CrossRef]
138. Wu, T.; Gao, X.J.; Ge, F.; Zheng, H.G. Metal–organic frameworks (MOFs) as fluorescence sensors: Principles, development and prospects. *CrystEngComm* **2022**, *24*, 7881–7901. [CrossRef]
139. Wang, Y.; Wang, L.; Huang, W.; Zhang, T.; Hu, X.; Perman, J.A.; Ma, S. A metal–organic framework and conducting polymer based electrochemical sensor for high performance cadmium ion detection. *J. Mater. Chem. A* **2017**, *5*, 8385–8393. [CrossRef]
140. Chen, M.; Xu, W.-M. An Anionic Calcium Metal–Organic Framework Encapsulated with TbIII Ions as a Recyclable Luminescent Sensor for CrIII and FeIII Ions. *Aust. J. Chem.* **2019**, *72*, 910–915. [CrossRef]
141. Zhan, Z.; Liang, X.; Zhang, X.; Jia, Y.; Hu, M. A water-stable europium-MOF as a multifunctional luminescent sensor for some trivalent metal ions (Fe^{3+} , Cr^{3+} , Al^{3+}), PO $^{4-}_4$ 3-ions, and nitroaromatic explosives. *Dalton Trans.* **2019**, *48*, 1786–1794. [CrossRef]
142. Sun, Z.; Yang, M.; Ma, Y.; Li, L. Multi-Responsive Luminescent Sensors Based on Two-Dimensional Lanthanide–Metal Organic Frameworks for Highly Selective and Sensitive Detection of Cr(III) and Cr(VI) Ions and Benzaldehyde. *Cryst. Growth Des.* **2017**, *17*, 4326–4335. [CrossRef]

143. Shi, W.; He, M.; Li, W.; Wei, X.; Bui, B.; Chen, M.; Chen, W. Cu-Based Metal–Organic Framework Nanoparticles for Sensing Cr(VI) Ions. *ACS Appl. Nano Mater.* **2021**, *4*, 802–810. [[CrossRef](#)]
144. Liu, Z.; Cui, T.; Pulletikurthi, G.; Lahiri, A.; Carstens, T.; Olszewski, M.; Endres, F. Dendrite-Free Nanocrystalline Zinc Electrodeposition from an Ionic Liquid Containing Nickel Triflate for Rechargeable Zn-Based Batteries. *Angew. Chem. Int. Ed. Engl.* **2016**, *55*, 2889–2893. [[CrossRef](#)] [[PubMed](#)]
145. Lin, X.; Gao, G.; Zheng, L.; Chi, Y.; Chen, G. Encapsulation of Strongly Fluorescent Carbon Quantum Dots in Metal–Organic Frameworks for Enhancing Chemical Sensing. *Anal. Chem.* **2013**, *86*, 1223–1228. [[CrossRef](#)]
146. Liu, S.; Li, J.; Luo, F. The first transition-metal metal–organic framework showing cation exchange for highly selectively sensing of aqueous Cu(II) ions. *Inorg. Chem. Commun.* **2010**, *13*, 870–872. [[CrossRef](#)]
147. Jayaramulu, K.; Narayanan, R.P.; George, S.J.; Maji, T.K. Luminescent microporous metal–organic framework with functional lewis basic sites on the pore surface: Specific sensing and removal of metal ions. *Inorg. Chem.* **2012**, *51*, 10089–10091. [[CrossRef](#)]
148. Zheng, T.T.; Zhao, J.; Fang, Z.W.; Li, M.T.; Sun, C.Y.; Li, X.; Wang, X.L.; Su, Z.M. A luminescent metal organic framework with high sensitivity for detecting and removing copper ions from simulated biological fluids. *Dalton Trans.* **2017**, *46*, 2456–2461. [[CrossRef](#)] [[PubMed](#)]
149. Li, H.; He, Y.; Li, Q.; Li, S.; Yi, Z.; Xu, Z.; Wang, Y. Highly sensitive and selective fluorescent probe for Fe³⁺ and hazardous phenol compounds based on a water-stable Zn-based metal–organic framework in aqueous media. *RSC Adv.* **2017**, *7*, 50035–50039. [[CrossRef](#)]
150. Zhao, S.S.; Yang, J.; Liu, Y.Y.; Ma, J.F. Fluorescent Aromatic Tag-Functionalized MOFs for Highly Selective Sensing of Metal Ions and Small Organic Molecules. *Inorg. Chem.* **2016**, *55*, 2261–2273. [[CrossRef](#)]
151. Wu, Y.; Wu, J.; Luo, Z.; Wang, J.; Li, Y.; Han, Y.; Liu, J. Fluorescence detection of Mn²⁺, Cr²O₇²⁻ and nitroexplosives and photocatalytic degradation of methyl violet and rhodamine B based on two stable metal–organic frameworks. *RSC Adv.* **2017**, *7*, 10415–10423. [[CrossRef](#)]
152. Li, L.; Shen, S.; Lin, R.; Bai, Y.; Liu, H. Rapid and specific luminescence sensing of Cu(ii) ions with a porphyrinic metal–organic framework. *Chem. Commun.* **2017**, *53*, 9986–9989. [[CrossRef](#)] [[PubMed](#)]
153. Hou, B.L.; Tian, D.; Liu, J.; Dong, L.Z.; Li, S.L.; Li, D.S.; Lan, Y.Q. A Water-Stable Metal-Organic Framework for Highly Sensitive and Selective Sensing of Fe³⁺ Ion. *Inorg. Chem.* **2016**, *55*, 10580–10586. [[CrossRef](#)] [[PubMed](#)]
154. Chen, S.; Shi, Z.; Qin, L.; Jia, H.; Zheng, H. Two New Luminescent Cd(II)-Metal–Organic Frameworks as Bifunctional Chemosensors for Detection of Cations Fe³⁺, Anions CrO₄²⁻, and Cr₂O₇²⁻ in Aqueous Solution. *Cryst. Growth Des.* **2016**, *17*, 67–72. [[CrossRef](#)]
155. Gai, Y.L.; Guo, Q.; Zhao, X.Y.; Chen, Y.; Liu, S.; Zhang, Y.; Zhuo, C.X.; Yao, C.; Xiong, K.C. Extremely stable europium-organic framework for luminescent sensing of Cr₂O₇²⁻ and Fe³⁺ in aqueous systems. *Dalton Trans.* **2018**, *47*, 12051–12055. [[CrossRef](#)] [[PubMed](#)]
156. Wang, B.; Yang, Q.; Guo, C.; Sun, Y.; Xie, L.H.; Li, J.R. Stable Zr(IV)-Based Metal-Organic Frameworks with Predesigned Functionalized Ligands for Highly Selective Detection of Fe(III) Ions in Water. *ACS Appl. Mater. Interfaces* **2017**, *9*, 10286–10295. [[CrossRef](#)] [[PubMed](#)]
157. Liu, C.; Yan, B. A novel photofunctional hybrid material of pyrene functionalized metal–organic framework with conformation change for fluorescence sensing of Cu²⁺. *Sens. Actuators B Chem.* **2016**, *235*, 541–546. [[CrossRef](#)]
158. Jin, J.; Yang, G.; Liu, Y.; Cheng, S.; Liu, J.; Wu, D.; Wang, Y.Y. Two Series of Microporous Lanthanide-Organic Frameworks with Different Secondary Building Units and Exposed Lewis Base Active Sites: Sensing, Dye Adsorption, and Magnetic Properties. *Inorg. Chem.* **2019**, *58*, 339–348. [[CrossRef](#)] [[PubMed](#)]
159. Jin, J.; Xue, J.; Liu, Y.; Yang, G.; Wang, Y.Y. Recent progresses in luminescent metal–organic frameworks (LMOFs) as sensors for the detection of anions and cations in aqueous solution. *Dalton Trans.* **2021**, *50*, 1950–1972. [[CrossRef](#)] [[PubMed](#)]
160. Rath, B.B.; Vittal, J.J. Water Stable Zn(II) Metal-Organic Framework as a Selective and Sensitive Luminescent Probe for Fe(III) and Chromate Ions. *Inorg. Chem.* **2020**, *59*, 8818–8826. [[CrossRef](#)]
161. Xu, R.X.; Yu, X.Y.; Gao, C.; Jiang, Y.J.; Han, D.D.; Liu, J.H.; Huang, X.J. Non-conductive nanomaterial enhanced electrochemical response in stripping voltammetry: The use of nanostructured magnesium silicate hollow spheres for heavy metal ions detection. *Anal. Chim. Acta* **2013**, *790*, 31–38. [[CrossRef](#)]
162. Lim, K.S.; Jeong, S.Y.; Kang, D.W.; Song, J.H.; Jo, H.; Lee, W.R.; Phang, W.J.; Moon, D.; Hong, C.S. Luminescent Metal-Organic Framework Sensor: Exceptional Cd²⁺ Turn-On Detection and First In Situ Visualization of Cd²⁺ Ion Diffusion into a Crystal. *Chemistry* **2017**, *23*, 4803–4809. [[CrossRef](#)] [[PubMed](#)]
163. Li, Q.; Wang, C.; Tan, H.; Tang, G.; Gao, J.; Chen, C.H. A turn on fluorescent sensor based on lanthanide coordination polymer nanoparticles for the detection of mercury(ii) in biological fluids. *RSC Adv.* **2016**, *6*, 17811–17817. [[CrossRef](#)]
164. Lin, X.; Luo, F.; Zheng, L.; Gao, G.; Chi, Y. Fast, sensitive, and selective ion-triggered disassembly and release based on tris(bipyridine)ruthenium(II)-functionalized metal–organic frameworks. *Anal. Chem.* **2015**, *87*, 4864–4870. [[CrossRef](#)]
165. Wang, P.; Ma, J.P.; Dong, Y.B.; Huang, R.Q. Tunable luminescent lanthanide coordination polymers based on reversible solid-state ion-exchange monitored by ion-dependent photoinduced emission spectra. *J. Am. Chem. Soc.* **2007**, *129*, 10620–10621. [[CrossRef](#)] [[PubMed](#)]
166. Lin, X.; Hong, Y.; Zhang, C.; Huang, R.; Wang, C.; Lin, W. Pre-concentration and energy transfer enable the efficient luminescence sensing of transition metal ions by metal–organic frameworks. *Chem. Commun.* **2015**, *51*, 16996–16999. [[CrossRef](#)]

167. Burtch, N.C.; Jasuja, H.; Walton, K.S. Water stability and adsorption in metal-organic frameworks. *Chem. Rev.* **2014**, *114*, 10575–10612. [[CrossRef](#)]
168. He, W.; Ifraimov, R.; Raslin, A.; Hod, I. Room-Temperature Electrochemical Conversion of Metal–Organic Frameworks into Porous Amorphous Metal Sulfides with Tailored Composition and Hydrogen Evolution Activity. *Adv. Funct. Mater.* **2018**, *28*, 1707244. [[CrossRef](#)]
169. Hendon, C.H.; Tiana, D.; Walsh, A. Conductive metal-organic frameworks and networks: Fact or fantasy? *Phys. Chem. Chem. Phys.* **2012**, *14*, 13120–13132. [[CrossRef](#)] [[PubMed](#)]
170. Yuan, S.; Qin, J.S.; Lollar, C.T.; Zhou, H.C. Stable Metal-Organic Frameworks with Group 4 Metals: Current Status and Trends. *ACS Cent. Sci.* **2018**, *4*, 440–450. [[CrossRef](#)]
171. Gkaniatsou, E.; Sicard, C.E.M.; Ricoux, R.E.M.; Mahy, J.P.; Steunou, N.; Serre, C. Metal–organic frameworks: A novel host platform for enzymatic catalysis and detection. *Mater. Horiz.* **2017**, *4*, 55–63. [[CrossRef](#)]
172. Gu, C.; Guo, C.; Li, Z.; Wang, M.; Zhou, N.; He, L.; Zhang, Z.; Du, M. Bimetallic ZrHf-based metal-organic framework embedded with carbon dots: Ultra-sensitive platform for early diagnosis of HER2 and HER2-overexpressed living cancer cells. *Biosens. Bioelectron.* **2019**, *134*, 8–15. [[CrossRef](#)] [[PubMed](#)]
173. Niu, X.; Li, X.; Lyu, Z.; Pan, J.; Ding, S.; Ruan, X.; Zhu, W.; Du, D.; Lin, Y. Metal-organic framework based nanozymes: Promising materials for biochemical analysis. *Chem. Commun.* **2020**, *56*, 11338–11353. [[CrossRef](#)] [[PubMed](#)]
174. Niu, X.; Shi, Q.; Zhu, W.; Liu, D.; Tian, H.; Fu, S.; Cheng, N.; Li, S.; Smith, J.N.; Du, D.; et al. Unprecedented peroxidase-mimicking activity of single-atom nanozyme with atomically dispersed Fe-Nx moieties hosted by MOF derived porous carbon. *Biosens. Bioelectron.* **2019**, *142*, 111495. [[CrossRef](#)] [[PubMed](#)]
175. Jiao, L.; Yan, H.; Wu, Y.; Gu, W.; Zhu, C.; Du, D.; Lin, Y. When Nanozymes Meet Single-Atom Catalysis. *Angew. Chem. Int. Ed.* **2020**, *59*, 2565–2576. [[CrossRef](#)]
176. Lin, T.; Qin, Y.; Huang, Y.; Yang, R.; Hou, L.; Ye, F.; Zhao, S. A label-free fluorescence assay for hydrogen peroxide and glucose based on the bifunctional MIL-53(Fe) nanozyme. *Chem. Commun.* **2018**, *54*, 1762–1765. [[CrossRef](#)]
177. Ye, K.; Wang, L.; Song, H.; Li, X.; Niu, X. Bifunctional MIL-53(Fe) with pyrophosphate-mediated peroxidase-like activity and oxidation-stimulated fluorescence switching for alkaline phosphatase detection. *J. Mater. Chem. B* **2019**, *7*, 4794–4800. [[CrossRef](#)] [[PubMed](#)]
178. Zhang, J.; Han, J.; Li, H.; Li, Z.; Zou, P.; Li, J.; Zhao, T.; Che, J.; Yang, Y.; Yang, M.; et al. Lymphocyte Membrane- and 12p1-Dual-Functionalized Nanoparticles for Free HIV-1 Trapping and Precise siRNA Delivery into HIV-1-Infected Cells. *Adv. Sci.* **2023**, *10*, 2300282. [[CrossRef](#)] [[PubMed](#)]
179. Chandio, I.; Ai, Y.; Wu, L.; Liang, Q. Recent progress in MOFs-based nanozymes for biosensing. *Nano Res.* **2023**, *17*, 39–64. [[CrossRef](#)]
180. Li, X.; Wang, L.; Du, D.; Ni, L.; Pan, J.; Niu, X. Emerging applications of nanozymes in environmental analysis: Opportunities and trends. *Trac-Trends Anal. Chem.* **2019**, *120*, 115653. [[CrossRef](#)]
181. Giunchedi, P.; Conte, U. Spray-drying as a preparation method of microparticulate drug-delivery systems—An overview. *STP Pharma Sci.* **1995**, *5*, 276–290.
182. Okuyama, K.; Abdullah, M.; Lenggoro, I.W.; Iskandar, F. Preparation of functional nanostructured particles by spray drying. *Adv. Powder Technol.* **2006**, *17*, 587–611. [[CrossRef](#)]
183. Thiele, J.; Windbergs, M.; Abate, A.R.; Trebbin, M.; Shum, H.C.; Forster, S.; Weitz, D.A. Early development drug formulation on a chip: Fabrication of nanoparticles using a microfluidic spray dryer. *Lab A Chip* **2011**, *11*, 2362–2368. [[CrossRef](#)]
184. Rivas-Murias, B.; Fagnard, J.F.; Vanderbemden, P.; Traianidis, M.; Henrist, C.; Cloots, R.; Vertruyen, B. Spray drying: An alternative synthesis method for polycationic oxide compounds. *J. Phys. Chem. Solids* **2011**, *72*, 158–163. [[CrossRef](#)]
185. Troyano, J.; Camur, C.; Garzon-Tovar, L.; Carné-Sánchez, A.; Imaz, I.; Maspoch, D. Spray-Drying Synthesis of MOFs, COFs, and Related Composites. *Acc. Chem. Res.* **2020**, *53*, 1206–1217. [[CrossRef](#)]
186. Chaemchuen, S.; Zhou, K.; Mousavi, B.; Ghadamyari, M.; Heynderickx, P.M.; Zhuiykov, S.; Yusubov, M.S.; Verpoort, F. Spray drying of zeolitic imidazolate frameworks: Investigation of crystal formation and properties. *CrystEngComm* **2018**, *20*, 3601–3608. [[CrossRef](#)]
187. Daro, N.; Moulet, L.; Penin, N.; Paradis, N.; Létard, J.F.; Lebraud, E.; Buffière, S.; Chastanet, G.; Guionneau, P. Spray-Drying to Get Spin-Crossover Materials. *Materials* **2017**, *10*, 60. [[CrossRef](#)]
188. Wang, Z.; Ananias, D.; Carné-Sánchez, A.; Brites, C.D.; Imaz, I.; Maspoch, D.; Rocha, J.; Carlos, L.D. Lanthanide-Organic Framework Nano thermometers Prepared by Spray-Drying. *Adv. Funct. Mater.* **2015**, *25*, 2824–2830. [[CrossRef](#)]
189. Guillerm, V.; Garzon-Tovar, L.; Yazdi, A.; Imaz, I.; Juanhuix, J.; Maspoch, D. Continuous One-Step Synthesis of Porous M-XF6-Based Metal-Organic and Hydrogen-Bonded Frameworks. *Chemistry* **2017**, *23*, 6829–6835. [[CrossRef](#)] [[PubMed](#)]
190. Garzón-Tovar, L.; Cano-Sarabia, M.; Carné-Sánchez, A.; Carbonell, C.; Imaz, I.; Maspoch, D. A spray-drying continuous-flow method for simultaneous synthesis and shaping of microspherical high nuclearity MOF beads. *React. Chem. Eng.* **2016**, *1*, 533–539. [[CrossRef](#)]
191. Avci-Camur, C.; Troyano, J.; Pérez-Carvajal, J.; Legrand, A.; Farrusseng, D.; Imaz, I.; Maspoch, D. Aqueous production of spherical Zr-MOF beads via continuous-flow spray-drying. *Green Chem.* **2018**, *20*, 873–878. [[CrossRef](#)]
192. Bayliss, P.A.; Ibarra, I.A.; Pérez, E.; Yang, S.; Tang, C.C.; Poliakoff, M.; Schröder, M. Synthesis of metal-organic frameworks by continuous flow. *Green Chem.* **2014**, *16*, 3796–3802. [[CrossRef](#)]

193. Tse, J.Y.; Kadota, K.; Nakajima, T.; Uchiyama, H.; Tanaka, S.; Tozuka, Y. Crystalline Rearranged CD-MOF Particles Obtained via Spray-Drying Synthesis Applied to Inhalable Formulations with High Drug Loading. *Cryst. Growth Des.* **2022**, *22*, 1143–1154. [[CrossRef](#)]
194. Boix, G.; Han, X.; Imaz, I.; Maspoch, D. Millimeter-Shaped Metal-Organic Framework/Inorganic Nanoparticle Composite as a New Adsorbent for Home Water-Purification Filters. *ACS Appl. Mater. Interfaces* **2021**, *13*, 17835–17843. [[CrossRef](#)] [[PubMed](#)]
195. Chen, S.; Xing, Y.; Liu, X.; Zhao, L. Numerical investigation of the effect of the injection angle on the spray structures of an air-blast atomizer. *Eng. Comput.* **2020**, *38*, 2048–2077. [[CrossRef](#)]
196. Zhao, H.; Wu, Z.W.; Li, W.F.; Xu, J.L.; Liu, H.F. Nonmonotonic Effects of Aerodynamic Force on Droplet Size of Prefilming Air-Blast Atomization. *Ind. Eng. Chem. Res.* **2018**, *57*, 1726–1732. [[CrossRef](#)]
197. Diels, A.M.J.; Michiels, C.W. High-Pressure Homogenization as a Non-Thermal Technique for the Inactivation of Microorganisms. *Crit. Rev. Microbiol.* **2006**, *32*, 201–216. [[CrossRef](#)] [[PubMed](#)]
198. Li, Y.; Yin, H.; Wu, C.; He, J.; Wang, C.; Ren, B.; Wang, H.; Geng, D.; Zhang, Y.; Zhao, L. Preparation and in vivo evaluation of an intravenous emulsion loaded with an aprepitant-phospholipid complex. *Drug Deliv.* **2023**, *30*, 2183834. [[CrossRef](#)] [[PubMed](#)]
199. Xie, F.; Zhang, W.; Lan, X.; Gong, S.; Wu, J.; Wang, Z. Effects of high hydrostatic pressure and high pressure homogenization processing on characteristics of potato peel waste pectin. *Carbohydr. Polym.* **2018**, *196*, 474–482. [[CrossRef](#)]
200. Sun, Y.; Su, S.; Han, L.; Jiang, S. Development of a combining sterilization equipment of high pressure carbon dioxide treatment and ultra-high pressure homogenization treatment. *Food Mach.* **2017**, *33*, 84–86. [[CrossRef](#)]
201. Zhang, L.; Li, X.; Xu, X.; Song, L.; Bi, A.; Wu, C.; Ma, Y.; Du, M. Semisolid medium internal phase emulsions stabilized by dendritic-like mushroom cellulose nanofibrils: Concentration effect and stabilization mechanism. *Food Chem.* **2024**, *436*, 137693. [[CrossRef](#)]
202. Yu, Y.; Saleh, A.S.; Sun, X.; Wang, Z.; Lu, Y.; Zhang, D.; Zhang, C. Exploring the interaction between myofibrillar proteins and pyrazine compounds: Based on molecular docking, molecular dynamics simulation, and multi-spectroscopy techniques. *Int. J. Biol. Macromol.* **2023**, *253*, 126844. [[CrossRef](#)] [[PubMed](#)]
203. Hou, J.; Xu, H.N. Ejected microcrystals probe jammed states of droplets in cyclodextrin-based emulsions. *Carbohydr. Polym.* **2024**, *324*, 121455. [[CrossRef](#)] [[PubMed](#)]
204. Lopes, R.P.; Mota, M.J.; Gomes, A.M.; Delgadillo, I.; Saraiva, J.A. Application of High Pressure with Homogenization, Temperature, Carbon Dioxide, and Cold Plasma for the Inactivation of Bacterial Spores: A Review. *Compr. Rev. Food Sci. Food Saf.* **2018**, *17*, 532–555. [[CrossRef](#)] [[PubMed](#)]
205. Chevalier-Lucia, D.; Picart-Palmade, L.; Dumay, E. Current trends in research and applications of dynamic high-pressure. *J. Phys. Conf. Ser.* **2017**, *950*, 032007. [[CrossRef](#)]
206. Biswal, B.P.; Chandra, S.; Kandambeth, S.; Lukose, B.; Heine, T.; Banerjee, R. Mechanochemical Synthesis of Chemically Stable Isoreticular Covalent Organic Frameworks. *J. Am. Chem. Soc.* **2013**, *135*, 5328–5331. [[CrossRef](#)] [[PubMed](#)]
207. Karak, S.; Kandambeth, S.; Biswal, B.P.; Sasmal, H.S.; Kumar, S.; Pachfule, P.; Banerjee, R. Constructing Ultraporous Covalent Organic Frameworks in Seconds via an Organic Terracotta Process. *J. Am. Chem. Soc.* **2017**, *139*, 1856–1862. [[CrossRef](#)]
208. Nechyporchuk, O.; Belgacem, M.N.; Bras, J. Production of cellulose nanofibrils: A review of recent advances. *Ind. Crops Prod.* **2016**, *93*, 2–25. [[CrossRef](#)]

Disclaimer/Publisher's Note: The statements, opinions and data contained in all publications are solely those of the individual author(s) and contributor(s) and not of MDPI and/or the editor(s). MDPI and/or the editor(s) disclaim responsibility for any injury to people or property resulting from any ideas, methods, instructions or products referred to in the content.